Response to Anonymous Referees,

The Green Ocean: Precipitation Insights from the GoAmazon2014/5 Experiment

Die Wang et al.

The authors would like to thank all reviewers for their helpful comments and suggestions. We have responded to all reviewers in a single document. As a brief summary, the revisions to the manuscript include the following highlights:

- We have modified several of the previous images (fonts, lines, sizing, labels, etc.)
- The manuscript has incorporated several changes in response to reviewer comments.
- Additional supplemental materials have been provided, including six figures, and used to relocate previous Table 3.

The individual reviewer comments and responses are included in the following document (author comments in black, reviewer comments in grey and italics).

Response to Anonymous Referee #1

Overall: This paper looks at precipitation characteristics during the GoAmazon2014/5 campaign using coupled RWP and disdrometer measurements. The study has the aims of improving our 1) interpretation of radar rainfall relationships, 2) understanding of DSD differences between wet/dry seasons and convective/stratiform regimes, 3) understanding of the possible role of polluted/clean regimes in invigorating convection, and 4) concept of the 'Green Ocean' with the previous points taken as context. There are many angles to this study, and overall it does a good job of addressing the above points. The language and flow of the paper, along with how 'in-depth' the discussion was, greatly improved as the paper progressed; I think it would be beneficial to flesh out some of the discussion in sections 3-4, improve the structure/flow of some of the paragraphs, and clean up some of the figures.

We thank the reviewer for their kind words. We hope our revisions are sufficient to address many concerns of this reviewer.

Introduction
This section successfully highlights the motivations and benefits of studying precipitation properties using data from the GoAmazon2014/5 campaign; however, certain sentences/paragraphs seem to be more elaborate repetitions of previous ones (see the following in-depth comments for examples). Concisely rephrasing some parts may make this section less wordy and easier to parse through. Overall, it does do a good job of summarizing the many different angles/benefits this study will have.

P2 L2-6 "diverse forcing conditions" is vague; sentences could be restructured, as it seems a bit circular/hard to follow

Agree with the reviewer. Replacing the line, "Thus, improving precipitation measurements (i.e., those that better reflect the natural variability of clouds under diverse forcing conditions) has traditionally supported improved convective treatments."

With,

"Thus, a traditional observational approach in support of convective modeling has been to document global precipitation variability and improve basic rainfall retrievals."

P2 L9-11 This is a bit repetitive of the previous paragraphs; could integrate together somehow.

Agree. Can drop the line (and references), "The inability of GCMs to adequately represent cumulus clouds and precipitation over the Amazon highlights one example of the observational needs for future improvement to GCM cloud parameterizations and the larger-scale circulation connections therein (e.g., Richter and Xie, 2008; Nobre et al., 2009; Yin et al., 2013)"

P2 L11 "Low-level barrier" is a strange phrase to use?

Agree. Replaced line with, "One source of uncertainty when developing useful precipitation retrievals for model development is the shortage of long-term surface gauge and disdrometer observations within tropical regions."

P2 L13-15 Needs restructuring/rewording, seems out of place as it is now

Agree. Replaced, “Geophysical retrievals of interest for precipitation studies include radar-based rainfall estimation, but even basic radar preprocessing improvements for dual-polarization quantities can be critical for future studies utilizing forward radar model comparisons.”

With,

“Although radar rainfall estimation and its uncertainty for tropical applications is of primary interest, basic radar preprocessing, calibration and dual-polarization radar data quality is also improved with extended surface precipitation records in diverse environments.”

P2 L18 Mention that this is what was used in GoAmazon?

Agree. Changed the line to, “Establishing boundaries for tropical precipitation expectations and radar data quality concepts (e.g., Scarchilli et al., 1996, self-consistency methods) provides an immediate benefit when interpreting remote radar deployment datasets including those from the Atmospheric Radiation Measurement (Ackerman and Stokes, 2003, ARM) Mobile Facility (Miller et al., 2016, AMF) during GoAmazon2014/5.”

P2 L23-25 The “Green Ocean” terminology needs to be better defined
P2 L22-32 These set of sentences need to be restructured or rephrased, especially towards the latter lines

Revised the paragraph as, “Although improving hydrological retrievals is of a practical significance, an interesting outcome from previous Amazon studies is the labelling of the Amazon as the ‘Green Ocean’. This Green Ocean terminology is rooted in studies such as Roberts et al. (2001) wherein low cloud condensation nuclei (CCN) concentrations and high CCN to condensation nuclei (CN) ratios over the Amazon resembled marine environments, as distinct from previous continental expectations. However, this terminology is often extended to include the unique regional characteristics observed from Amazon convection that spans oceanic to continental cloud extremes in key attributes such as updraft intensities and propensity for electrification. Specific to convection, Amazon clouds may initiate under these clean (or lower) CCN conditions, over a pristine forest, but also experience a range of thermodynamical and aerosol forcing influences that promote changes in cloud properties including electrification, cloud droplet size distribution and precipitation changes, or enhanced updraft intensity (e.g., Williams et al., 2002; Cecchini et al., 2016; Giangrande et al., 2016b, 2017). As described by Williams et al. (2002), the prevalence of maritime convective cloud regimes over a large continent are possibly still underappreciated in the convective cloud spectrum and its intensity, especially given the propensity to identify deeper convection over the Amazon having electrification arguing continental convective characteristics.”

P2 L34-35 I am not sure what is being said in this sentence and would suggest rewording

Reworded to, “One motivation for this study is to identify conditions under which precipitation sampled in the Amazon basin adheres more towards oceanic, maritime and continental characteristics (e.g., Tokay and Short, 1996).”

P3 L4-5 This study seems pretty focused on just the GoAmazon dataset; is it accurate to say that you are looking at this in the context of global variability and shifts in this?

P3 L5 What is the benefit/meaning behind "(or, practical)"?

Here, reworded the line, "In addition to better addressing Amazon precipitation in the context of global variability, it is useful to assess whether traditional (or, practical) radar remote-sensing (including dual-polarization) quantities are sensitive to these shifts. "

To,

"While it is important to view these Amazon datasets and cloud or larger-scale regime shifts in the context of global disdrometer observations (e.g., Dolan et al. 2018), it is also useful to determine whether common remote-sensing platforms (e.g., dual-polarization quantities as from X-band to S-band radars) are sensitive to these differences."

P3 L10 Unnecessary "a" in "…capture a continuous convective cloud…"

Fixed, thanks.

Dataset and Methodology

I liked this section, 2.1 in particular gives a great overview of the total precipitation statistics embedded in a realistic idea of the associated uncertainties. The paper covers a lot, and the use of specific subsections made sure the reader was orientated properly. The main confusion for me is within the discussion for Figure 1, which could possibly use some clarification (see in-depth comments).

2.1 The ARM T3 Precipitation Dataset and Processing
Subtitle (and subsequent subtitles) Unnecessary "the"; this subsection also concerns the RWP, so not just the precipitation dataset?

Revised to 'ARM T3 Precipitation and Radar Wind Profiler Dataset and Processing'

P3 L29 Reference/reason for R>0.5 mmhr-1 and total drops > 100?

The drop count and rainfall rate thresholds help prevent small sample sizes from skewing DSD estimates (Smith et al. 1993; Smith 2016; Dolan et al. 2018). These thresholds are typically similar across most of the disdrometer literature (usually following Tokay recommendations, etc.), but could vary if the disdrometer dataset is processed for other time resolutions or for different locations sampling different types of precipitation. These values may also be different if the disdrometer is assumed of higher quality, e.g., 2D Video Disdrometers may allow for lower rainfall rates and/or drop count threshold owing to improved small drop size sampling. For example, in Park et al. (2017), this study processed the 1-min DSDs by removing data if the total number of drops was < 30 and R < 0.01 mmhr^{-1}. In regimes with high concentrations of smaller drops (e.g., orographic settings, drizzle), one may potentially implement an even higher drop count threshold.

Smith, P. L., Z. Liu, and J. Joss, 1993: A study of sampling-variability effects in raindrop size observations. J. Appl. Meteor., 32, 1259–1269

Smith, P. L., 2016: Sampling issues in estimating radar variables from disdrometer data. J. Atmos. Oceanic Technol., 33, 2305–2313

Dolan, B., B. Fuchs, S.A. Rutledge, E.A. Barnes, and E.J. Thompson, 2018: Primary Modes of Global Drop Size Distributions. J. Atmos. Sci., 75, 1453–1476

Park, S., H. Kim, Y. Ham, and S. Jung, 2017: Comparative Evaluation of the OTT PARSIVEL2 Using a Collocated Two-Dimensional Video Disdrometer. J. Atmos. Oceanic Technol., 34, 2059–2082

P4 L2 Missing "and" before listing the mass-weighted mean diameter

Fixed, thanks.

P4 L9 Comma missing after (degkm^{-1})

Fixed, thanks.

P4 L10 Why 20 degrees C?

We adopted 20C as it reflects a common assumption from the literature (to assist in relative alignment, comparisons). This assumption does not impact the estimates of Z or K_{DP} as significantly as it would A_h and relative relations therein. For A_h, we provide an additional reference for 10C, as is often reported for multiple temperatures in the literature, e.g., Ryzhkov et al. (2014), Diederich et al. (2015). If the reviewer (or readers of this response) is interested in additional temperature variability, those calculations are not difficult can be performed on request. The eventual ARM disdrometer Value Added Product (VAPs) releases from these efforts will also include a wider range of calculations than what is presented in this manuscript.

Diederich, M., A. Ryzhkov, C. Simmer, P. Zhang, and S. Trömel, 2015: Use of Specific Attenuation for Rainfall Measurement at X-Band Radar Wavelengths. Part I: Radar Calibration and Partial Beam Blockage Estimation. J. Hydrometeor., 16, **487–502.**

Ryzhkov, A., M. Diederich, P. Zhang, and C. Simmer, 2014: Potential Utilization of Specific Attenuation for Rainfall Estimation, Mitigation of Partial Beam Blockage, and Radar Networking. J. Atmos. Oceanic Technol., 31, **599–619.**

P4 L18 Is this from your RWP analysis? Or should there be a reference here?

Yes, this statement comes from our RWP analysis (see the figure below). This figure shows the mean Vertical Velocity profiles (in color) as a function of 10 dBZ Echo-Top Height (ETH). This plot is only showing convective locations as observed during GoAmazon2014/5. The ETH (x-axis) and actual height above the RWP (y-axis) line up reasonably, in that the mean convective cloud vertical velocity approaches 0 m/s at this relative altitude (falls along a 1-to-1 line to ~ 15 km).

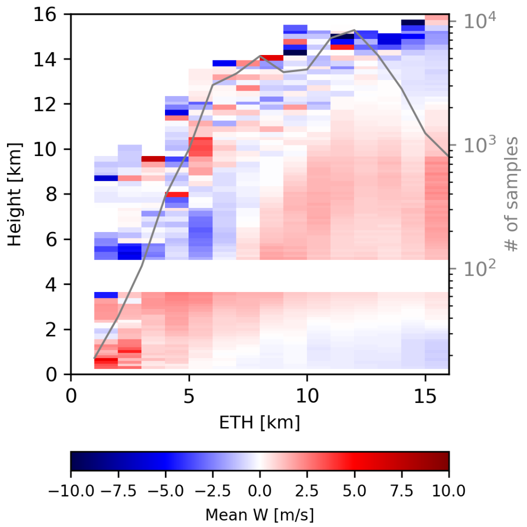

P4 L20-22 This seems like an incomplete sentence as you state "we first…" and do not follow it with anything else

Thanks. We have modified the sentence, "For echo classifications, we first identify higher confidence convective and stratiform regions on the basis of column Z signatures and/or so-called radar 'bright band' (melting-level) designations for longer wavelengths (e.g., Fabry and Zawadzki, 1995; Geerts and Dawei, 2004)."

To,

"For echo classifications, we identify convective and stratiform regions on the basis of column Z signatures, velocity properties, and/or so-called radar 'bright band' (melting-level) designations for longer wavelengths (e.g., Fabry and Zawadzki, 1995; Williams et al. 1995; Geerts and Dawei, 2004)."

P4 L30 "...aerosol classification is that each…"

Fixed, thanks.

P5 L4 The phase "and associated classifications" seems unnecessary

OK. We removed it.

P5 L5 "…potentially a factor of 3 or more…"

Agree. Thanks.

P5 L10-12 Are these from Thalman et al. (2017) again?

Yes.

P5 L21-22 Uncertainty in what? Radar quantities? Is there a way to provide a numerical value for the "variability established by previous studies" here?
P5 L22 Unnecessary "However,". Does the anticipated estimated uncertainty mentioned previously not include instrument offsets? These two sentences don't flow very well and could possibly do with some rearranging

Rephrase to: "Given our comparisons between rainfall accumulations with surface gauge measurements under typical storm intensities, as well as previous side-by-side performance testing of other PARSIVEL units, we do not anticipate radar quantity uncertainty falling outside the variability established by previous studies. For example, reasonable instrument offsets for radar quantities such as Z may be on the order of 10-20 % or 1-2 dBZ."

P5 L27-30 It may be beneficial to add a reference as to why 'b' is fixed and the variability of 'a' is tested

Ok. Have added a reference to:

Steiner, M., Smith, J. A. *and* Uijlenhoet, R. 2004 A microphysical interpretation of the radar reflectivity–rain rate relationship. J. Atmos. Sci., 61, 1114–1131

As, "As plotted in Figure 1, we show histograms for a-coefficient values from various single parameter rainfall relationships (radar quantities estimated as in previous sections), assuming a fixed b-coefficient as determined from our complete Amazon dataset for the S-band wavelength. This example highlights the sensitivity in the a-coefficients as estimated from random half-dataset subsets to the complete dataset (vertical black line). Assuming a constant b-coefficient ~1.4 is typically a reasonable assumption to assist in microphysical interpretation from R(Z) relationships for size-controlled conditions (e.g., Steiner et al. 2004)."

P5 L34 (Figure 1) For my clarification, Figure 1 is for the S-band wavelength, yet the discussion of the figure seems to include that of shorter wavelengths in comparison? Am I misinterpreting something here?

Yes, the discussions here are based on a- and b-coefficient distributions that we calculated for multiple wavelengths. Figure 1 only includes S-band shown as an example. We performed the same analysis for shorter wavelengths as well (see figures below for C and X-band), which are not shown in the manuscript, however we provide them below.

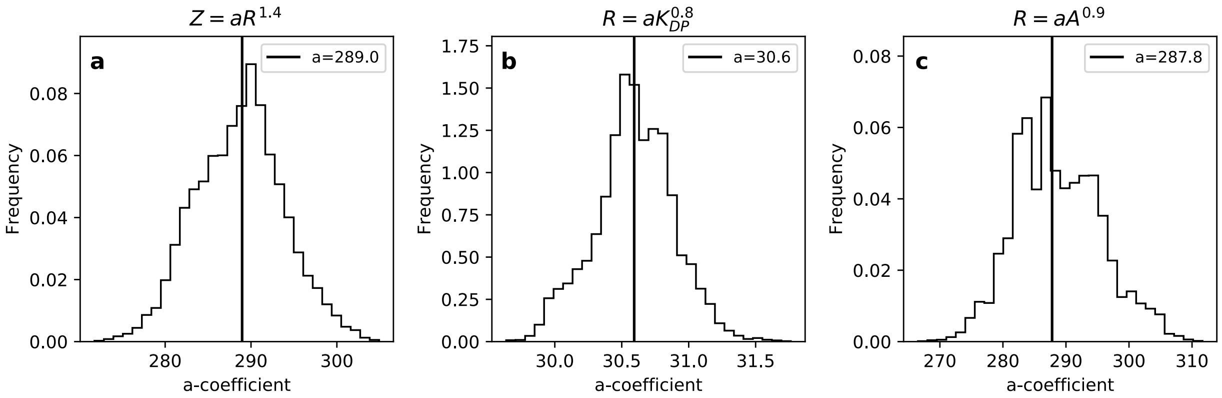

Figure S1: Histograms for a-coefficient values from single parameter rainfall relationships (a) R(Z), (b) $R(K_{DP})$, and (c) R(A), calculated using least square method under the assumption of a fixed b-coefficient from random sampling of half of the dataset (5000 times), for the C-band wavelength. The red curves represent the fit Gaussian distribution of a-coefficient. The red vertical lines represent the a-coefficient calculated based on the whole dataset.

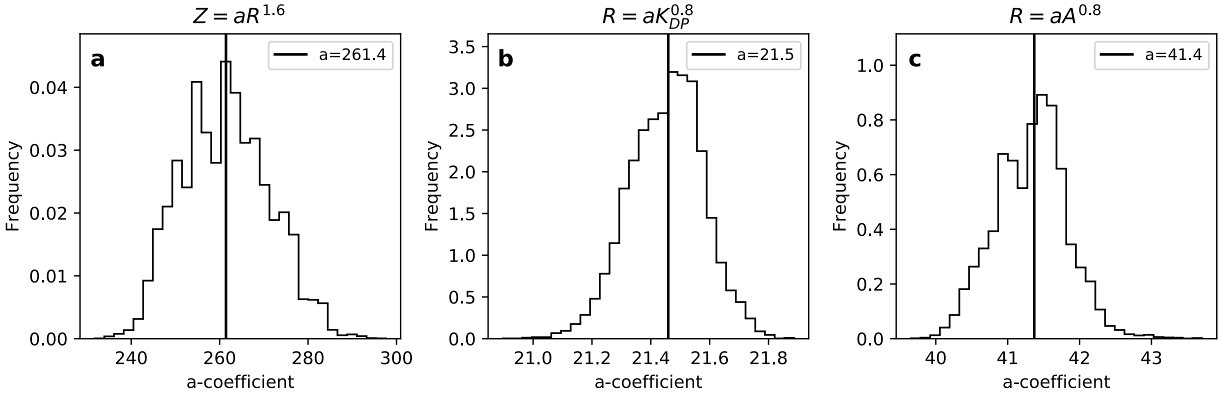

Figure S2: The same as Figure1 but for X-band wavelength.

We will rephrase the line to,

"Though not shown in Figure 1, a deterioration in performance at shorter wavelengths is found for R (Z) relationships owing to …. The corresponding plots for C-band and X-band are provided in the supplemental material (Figures S1 and S2)."

As above, since we are including supplemental material, these images can be included in that format as well.

P6 L9-11 Have you considered/is it possible to compare or mention possible datasets from a climate/region more comparable to the Amazon? SGP will obviously (and as acknowledged by yourselves) have differences to the Amazon even though it is continental, so do any datasets (even short term) exist for an even more relevant point of comparison? I do like how they both have similar processing, so I understand why this dataset is used and do not think it is unnecessary, but extra comparisons may be interesting

Having a Darwin component that expanded on Giangrande et al. (2014) ARM JWD insights was an initial plan for this manuscript (e.g., an improved tropical comparison with similar disdrometers as a callback to Tokay and Short, etc.). Unfortunately, at the time of writing, we did not have direct permission to the datasets from Darwin, Australia, e.g., those that have been collected by a higher quality 2DVD unit (approximately 5-year archive as established by Bringi and others). The ARM JWD impact disdrometer archive from Darwin was also a possibility, but that instrument type is usually considered of lower quality for dual-polarization efforts.

We have performed some comparisons with the Darwin datasets and find that the results from Darwin are quite similar to those from the Amazon in terms of applications for the Darwin C-band radars and associated rainfall and processing coefficient needs therein (e.g., deeper convection, monsoonal events). The most pronounced difference is in the lower frequency for these shallower/congestus contributions to the rainfall datasets.

Table 1 The AM and SGP abbreviations could be defined in the caption for completeness

OK, rephrased the caption of Table 1: …for All, Wet, and Dry seasons, for the Amazon (MAO) and the Southern Great Plains (SGP) sites". We changed AM to MAO to keep that consistent with the name of the dataset on ARM website.

P6 L7-16 I understand that you have addressed the reasons why there are differences elsewhere, but a sentence on the fact that a tropical vs midlatitude location would account for these differences may be worthwhile here. A lot of what is said here is expanded on in later sections – is this paragraph completely necessary?

We prefer to introduce each section with a brief summary, an author preference. We have added at the end of that paragraph, "Discrepancies between SGP and Amazon, as well as Wet/Dry separations, are most pronounced at the higher R consistent with convective cores. This is likely based on the propensity for melting hail in deeper SGP convection and/or larger melting aggregates in stratiform regions trailing convective lines favoring larger drop sizes at the surface."

Table 2 Is this better suited in supplemental material?

Possibly – However, we think that it is informative to include Table 2 in the main manuscript. We do agree with this reviewer and the second reviewer that the supplemental material option may be useful for Table 3 and to include other wavelength/important information.

P6 L21-22 SGP is a continental reference, but I think more emphasis should be on the comparison between latitudes instead

As to a previous reviewer comment, the 'continental' reference is useful when addressing prior 'Green Ocean' terminology and its applicability therein. We would have preferred to include an additional Darwin reference/contribution if a comparable dataset was available to us (we do not have permission and think this comparison would make a lengthy manuscript longer and detract from some of the other findings). Another option within DOE ARM was the Gan dataset as discussed by Thompson et al. (2015). We felt this dataset was more reflective of an 'oceanic' condition, and best illustrated by referring to the TM classification lines.

Figure 2 Is there any way to show wavelength differences on the same/additional figure? Several parts of the discussion reference wavelength differences and it may be nice to see them summarized in a figure.

This is an example where we can include those plots as part of the supplemental materials, e.g., Figures S3 and S4. We will include a line in the text that points to the supplemental materials for these figures.

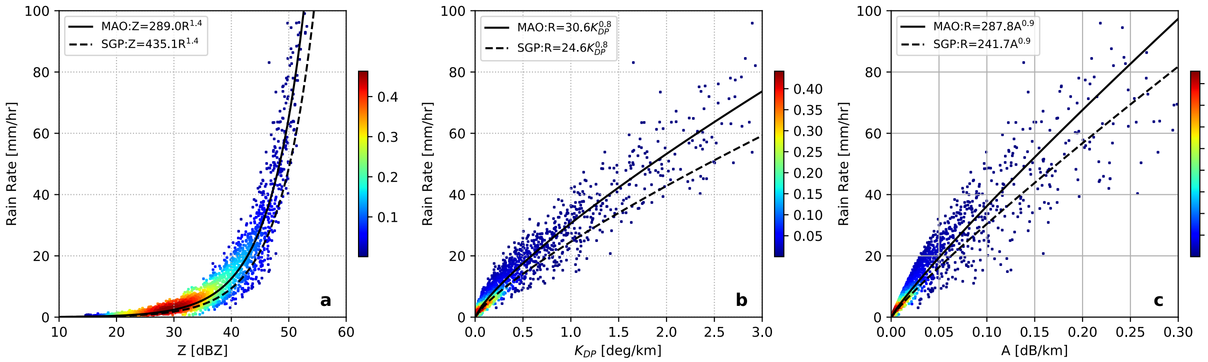

Figure S3. Scatter plots of (a) Z, (b) KDP, and (c) A versus rain rate and overlaid associated relationship fits using least square method for Amazon (MAO, solid lines) and SGP-Oklahoma (SGP, dashed lines) sites, for the C-band wavelength. Density is shown in color.

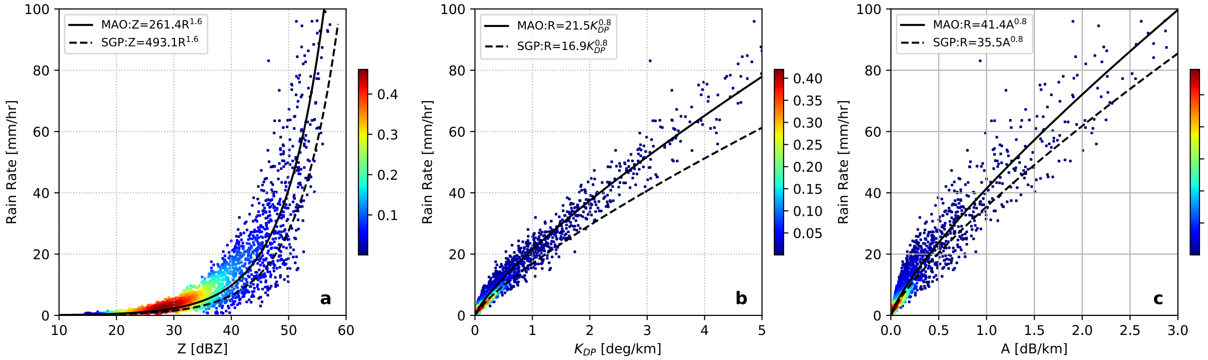

Figure S4. The same as Figure S3, but for X-band wavelength.

P6 L30-31 Would be nice to expand on this "significant change" a little here – what/why etc.

Added a better justification, e.g., larger than that expected from subsampling.

P7 L25 Have the authors considered restructuring to explain the convective/stratiform classification before analyzing the results of doing such here? I cannot find where the RWP classification is actually discussed. A few sentences of what the classification would be beneficial to the reader

In this case, we introduced the classification in the previous sections, but this may not have been clear. As in the section, the classification follows the previous Giangrande et. al. (2014;2016) RWP offerings, however we have added an extra reference in the above (Section 2.1) to Williams et al. (1995) – this was following a suggestion by C. Williams given the relative similarities of the RWP ideas to previous tropical RWP classification efforts he performed. To note, multiple authors have used very similar classification logic, e.g., identify meteorological from non-meteorological echo, identify convective cores, weaker convection from stratiform using precipitation and velocity signature thresholds, and typically a melting layer / bright band check to identify stronger stratiform signatures. The biggest change in this approach is that it starts by using a fuzzy logic approach as its initial backbone for echo identification – but, we still adopt some sanity checks / thresholds, ground precipitation checks, etc., to ensure reasonable echo identification. These efforts have also been improved, cross-checked with the availability of the collocated W-band (WACR) during GoAmazon2014/5 that is not sensitive to Bragg echo/insects.

Figure 3 This figure could be cleaned up. Consider moving the color bar for the top/bottom two plots outside of the main displays so it is less cluttered and can be seen more clearly.

Thanks. We have replotted the figure.

Figure 4 The white color assigned to the low probabilities is not easy to see when there is a white background. Furthermore, the color bar for these probabilities seems odd – is there any other way to present the probability legend (same problem with subsequent figures)? To make the captions clearer, I would address the shading and the dots separately in terms of what they represent

Agree. It should read 'Density' in the place of 'Probability'.

The differences between wet and dry seasons could be highlighted more in this section since it is an important aspect of the study. The findings on precipitation originating from congestus/shallower cloud systems is nontrivial, and the importance of this in context of the introduction could be emphasized more. I think explaining the RWP classification before now will help in latter parts of this section.

In this instance, we agree. We did not develop the Wet/Dry contrasts with much detail, perhaps since we (as authors) knew the more detailed DSD-driven Wet v Dry discussions would follow. This is also challenge when attempting to pack in the quantity of information while keeping certain concepts (e.g., rainfall relations) separate from more detailed (DSD) discussions. Our first thought is to simply acknowledge this to the reader, e.g., including the line - "Nevertheless, summary rainfall properties skew heavily towards convective designations for all seasons, as reported in Table S1. Seasonal changes will be discussed further in Section 4 in the context of multiparameter DSD breakdowns."

Figure 5 I like this figure, but the legend/labels in subplot c need to be fixed as the overlapping text is confusing/messy

Agree, we replotted Figure 5.

P8 L22 The fact that cloud top heights could extend 2 km above the heights shown seems a large difference. Can some comment be made about whether this is significant? Does this have any implications for the study or conclusions?

We include this statement (conservative) because these differences between RWP ETH and true CTH may be important for interpretation by future modeling activities (if those comparisons do not apply an appropriate forward radar simulator that can account for radar sensitivity considerations). In a relative sense, this does not have much of an impact, as our ETH criteria was driven by the naturally-occurring separation/bimodality in the ETH measurements from the RWP that is consistent with expected cloud top modes (e.g., Johnson et al. 1999, etc). However, the authors still wanted to note this potential uncertainty as there is an unknown difference between these ETH and cloud top height (same is true even for cloud radars having much higher sensitivity, on which these statements are rooted – having collocated WACR).

Johnson, R.H., T.M. Rickenbach, S.A. Rutledge, P.E. Ciesielski, and W.H. Schubert, 1999: Trimodal Characteristics of Tropical Convection. J. Climate, 12, 2397–2418,

P8 L22-24 What is the reasoning behind relating the winds during the wet/dry season to the modest values of Z in these sentences? Not a lot is said about subplot 5c and the need for highlighting the wind directions in the different seasons

Agree. Joined a sentence incorrectly. Should be rephrased as,

"Sounding-based winds over the T3 site are predominantly easterly (mostly observed during the Dry season) to northeasterly (mostly, Wet season) (Figure 5c). Low-level Z observations (Figure 5d) illustrate that Amazon cumulus are often linked to relatively modest values of Z ~ 35 dBZ."

P9 L3 What is meant by "magnitude exceeding threshold as on Figure 6"?

e.g., when the Vertical Velocity is greater than certain values (like 1 m/s, 3 m/s, and 5 m/s on the plot). We have removed this as it seems confusing.

P9 L29-30 I agree that the use of BR would minimize the contributions of shallower organized convection – but I am unsure of the applications of this given that a large portion of deeper organized convection also falls to the left of the BR line

We would agree that the main point is to show that a substantial portion of 'convective' clouds would still have DSDs that fall to the left of that separation line.

Figure 8 Should re-label the dashed and solid lines (BR/TM)

OK, we have re-labeled BR and TM lines on Figures 8, 9, 10, 11, 13, 15, and 16.

P10 L3 I am not sure what the phrase "orients this dataset in BR/TM formulation spaces to the left of the BR line" means. Also, more explanation of how this figure was produced may be necessary.
P10 L5-6 Looking at Figures 8a/c, it isn't obvious that contributions to the histogram are oceanic. I.e. DSDs are not significantly above the dashed TM line. The argument looks more solid for those DSDs identified as stratiform by the RWP

Agree. This should read,

"As plotted in Figure 8, we consider only the DSDs that would fall to the left of the BR separation line (e.g., those that follow a traditional BR stratiform designation). For this figure, the DSDs identified as belonging to convective or stratiform (based on the RWP definitions) are then subset according to the left and right panels, respectively."

As for the second comment, one can see from Figure 8a that a relative large portion of RWP-convective DSDs fall into/near Thompson oceanic concepts (smaller drops, higher number concentration). The argument is to highlight that there are Amazon convective and stratiform expectations from DSDs that would otherwise be described as 'stratiform' according to BR. The reviewer is correct in the sense of that we do have several DSDs near/below the Thompson TM line, which may be associated with echoes from transitions from convective to stratiform, etc. The RWP designating those areas as convection may simply indicate that regions aloft exhibited convective signatures or these are transitional regions at the periphery of convective regions. Again, the intent was not that all smaller drop or weaker convective Amazon DSDs would be found above this TM line (that would suggest all Amazon cloud-precipitation as

oceanic), but that a large % were consistent with oceanic properties as well. We would agree that the two 'stratiform' criteria usually implies DSDs clusters are below the Thompson line.

P10 L11 Again, need some discussion previous to this to back up why this is assumed to be a reasonably proxy

OK. Here, this choice is based on the bimodal distribution of ETH from Figure 5 and the associated discussion, fixes therein.

P10 L14-15 "Deeper cumulus clouds are associated with additional maritime continental DSD properties as similar to Darwin studies" – I look at Figure 9a, and I am not sure I see where this comes from. It is not obvious to me that a significant portion is to the right of the BR line, at least not relative to Figure 9b.

In these examples, we would agree that there is overlap between the two plots. However, this statement (maritime convective) is not necessarily used to imply that additional convection is to the 'right' of this BR line, but that fewer convective observations are found 'above' the TM 'oceanic' line. However, we do also find that there are larger-drop convective extremes, as well as additional evidence for more mature stratiform DSDs that are favoring aggregates (low N_w, higher D_0 observations).

P11 L2 An expansion on the discussion on Table 3 should either be given, or perhaps move this table to supplemental material. Not much is said about it here and it gets overlooked

As discussed with Table 2, it is possible to move this table (which was provided for statistical completeness) to supplemental materials (e.g., as Table S1). We think this change is reasonable and is more appropriate than moving Table 1.

Figure 13 Nothing is written in the text about the transitional period.

We would agree (e.g., Figures 10 and 13) minimal text was provided on the Transitional season (MON), and these images were provided for completeness. The months did tend to reflect transitional behaviors between the Wet and Dry season properties. Interestingly, previous studies by the authors (e.g., Giangrande et al. 2016), as well as storm electrification literature, have suggested that many intense convective cells (as defined by updraft speeds) are sampled during Transitional periods (e.g., October, November). In our examples, the Transitional months do not demonstrate cumulative dataset precipitation behaviors/extremes outside the bounds of the Wet or Dry season properties (which may simply be that outlier examples are also not highlighted well by our cumulative plots).

P14 L8 "…role of aerosols in the following invigoration arguments"

Agree. Thanks.

Response to Anonymous Referee #2

The authors explore some of the precipitation events during the wet and dry season of the GoAmazon experiment and try to decouple the aerosol/thermodynamic characteristics of the precipitation in each regime, and whether or not and the extent to which the precipitation exhibits an oceanic "flavor," as the Amazon basin is often dubbed the "Green Ocean." The debate about aerosol vs. thermodynamic effects, especially with regards to the intensity of convection and the DSDs of convective regimes continues to rage, and the authors rightly note that the two effects are tightly coupled and it is difficult to disentangle the effects from each other. Still, this is thorough investigation and a nice summary of the precipitation tendencies of the convection over the Amazon and provides insight into the meteorological and instrumental goings-on of the GoAmazon campaign. I have one minor point to pick about the CAPE/CIN statistics presented. I also add a thorough list of line-by-line comments but they are largely about writing and style. Overall, very minor revisions.

We thank this reviewer for the comments and suggestions, and we hope we have improved the revised manuscript in ways that respond to any concerns from this reviewer and the other reviewer comments above.

Major Comments:

With particular regard to the statistical analysis in lines 17-23 on page 13, as the distributions of CAPE and CIN are not normal distributions, I feel like a lot of detail is lost in presenting the mean and standard deviations alone. Especially if I am to accept the comparisons made throughout this paragraph, when the differences in MUCAPE (for example) for the different subsets are only a few hundred J/kg/K apart, but the standard deviations are over a thousand, or for the MUCIN, where one standard deviation away from the mean is of the opposite sign, I find those comparisons to be shaky. Could perhaps you show us histograms of the distributions themselves? Or instead present quartiles, or 10%, 90% quantiles? I feel like those would be more representative of these populations.

This is a valid point, and something the authors have discussed with others who have performed similar aerosol-cloud studies (e.g., Varble 2018). Modest variability in CAPE/CIN can have a significant impact – and that even a few hundred J/kg/K (if that was even a reasonable assumption) is non-trivial. We agree that at a minimum, the authors should provide histograms of these MUCAPE and MUCIN (as for example, in supplemental materials as suggested by reviewer 1). These can be found below and also in Figure S5, with an additional line added to the manuscript to point to this image. We have also added in a set of histograms for the later MUCAPE/MUCIN breakdowns as a function of wind direction in Figure S6 (supplemental, see below image). We think this is also useful to show for the readers/reviewers.

Varble, A., 2018: Erroneous Attribution of Deep Convective Invigoration to Aerosol Concentration. J. Atmos. Sci., 75**, 1351–1368, https://doi.org/10.1175/JAS-D-17-0217.1**

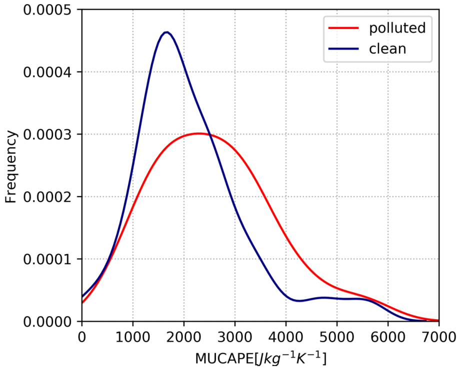

Figure 5S: Histograms of MUCAPE and MUCIN for polluted and clean cases.

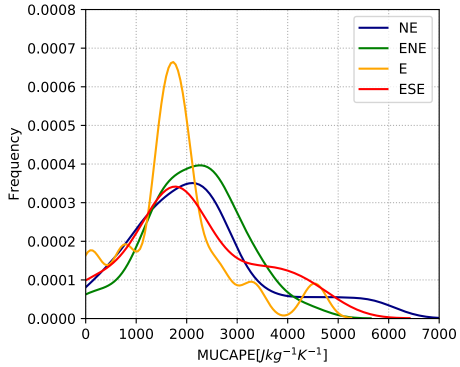

Figure 6S: Histograms of MUCAPE and MUCIN for different wind directions.

The figures in general are beautifully done. I think Figures 10, 13, and 15 might be easier to read if presented in one or two vertical columns, and the plot space of each panel increased. Similarly, it would be nice if the plot space of Figure 4b/c could be increased, as currently the detail of the blue contours is completely lost.

Yes, agree. We have modified the plots.

Throughout the text, there is a propensity to attribute verbs to the figure titles, as in "Figure 2 plots. . ." or "Figure 2 overlays. . . " While I take no issue with the instances in which you say "indicates," I reacted very strongly to the other instances where you are attributing action words to the figures themselves. I found it to be very distracting, and I suggest revising this throughout the text.

Ok, agree. We have revised several 'Figure * plots/presents/overlays/separates' and other instances throughout the text. These can be revised as suggested by the reviewer below.

Minor/Line-by-Line Comments:

1.16 "to better inform" is a split infinitive, and while manuals of style say that it has become perfectly acceptable to split an infinitive when justifiable, there are several of them throughout the text. Perhaps diversifying the verbiage, a little throughout the manuscript would help with the readability. This is a pedantic point, and you can keep the phrasing as-is, at your discretion.

Thank you for drawing this to our attention. We note many examples (esp. early on in the manuscript) such as ‘to better inform’, ‘to better constrain’, ‘to adequately represent’, ‘To better understand’, ‘to better addressing’, to further differentiate’, ‘to better isolate’. In most cases, we can easily remove the adverb (typically, the word ‘better’) and our point would be the same.

2.4 Suggest " . . . improving model capabilities introduces new challenges . . ."

Agree. Thanks.

2.7 do "observations" and "modeling" need to be capitalized?

Here, we think this use “Observations” and “Modeling” is appropriate for ACP as this seems to be the formal campaign name / use by the PI / overview article and other previous literature presents the official campaign naming in the ACP / special edition.

2.7 "were motivated"

Agree. Thanks.

2.10 "future improvement of GCMs"

Agree. Thanks.

2.11 "low-level barrier" when talking about circulation and dynamics is making me think of dynamic phenomena and not observation obstacles - can you rephrase?

Agree. This has been addressed as in following comments to Reviewer 1.

2.22 "are" does not agree with the subject "perspective" - this entire clause could use some rearranging for clarity.
2.24 Suggest " . . . regional characteristics of convection over the Amazon that spans oceanic . . ." 2.26 Suggest " . . . but may also experience a range of thermodynamic and aerosol . . ."
2.29 I believe the sentence should read "the prevalence . . . is underappreciated . . ." but also, the second clause of this sentence is confusing, suggest rephrasing.

Agree. Revised this paragraph as in following Reviewer 1 and Reviewer 2 comments.

2.34 Suggest "in order to identify" instead of "towards identifying"

Accepted. Thanks.

As in the Reviewer 1 response, reworded to, “One motivation for this study is to identify conditions under which precipitation sampled in the Amazon basin adheres more towards oceanic, maritime and continental characteristics (e.g., Tokay and Short, 1996).”

2.35 Suggest "trends" instead of "adheres"

Accepted. Thanks.

2.35 Suggest adding more text to "oceanic, maritime to continental characteristics." Maybe something like " . . . precipitation sampled in the Amazon basin trends more towards ocean, maritime characteristics, and when it trends towards possible continental characteristics." This might sound redundant but I had a hard time understanding where the logic of this sentence was going.

Accepted. Thanks.

3.9 Suggest " . . . and the possible effects of the Manaus, Brazil pollution plume."

Accepted. Thanks.

3.10 Suggest removing "a" from "a continuous convective cloud . . . "

Accepted. Thanks.

3.13 Suggest removing " . . . useful for future hydrological applications" I understand you are putting in the motivation for that section, but to say it here disrupts the flow of the sentence.

Accepted. Thanks.

3.23 Suggest "a period"

Accepted. Thanks.

4.27 Suggest "the number concentration". Also, the phrase "particles condensation nuclei" is confusing.

Rephrased as, "Aerosol regime classifications are based on the combination of condensation nuclei (CN) measurements, measurements for the fraction of particles with diameters less than 70 nm, and carbon monoxide CO and oxides of Nitrogen (NO_y) measurements at the T3 location using instrumentation as described in Thalman et al. (2017) and supplemental materials."

4.29 suggest "other supplemental materials"

Agree. Thanks.

5.3 suggest "values of"

Agree. Thanks.

5.5 suggest " . . . potentially a 3 or more factor of difference . . ."

Agree. Thanks.

5.30 onwards - suggest potentially writing coefficients as italicized letters, either by themselves, or with -coefficient, but the quote marks are awkward.

OK, changed to '*a*-coefficient' *for all the places.*

5.33 sensitivity to what?

Changed to 'sampling uncertainty'

6.4 " . . . basic interpretations of the significant changes . . ."

Accepted. Thanks.

6.11 "similarly"

Agree. Thanks.

6.14 why the hyphen in "higher-relative"

OK. Remove "-"

6.18 "Figure 2 plots . . ." this is the first instance of the Figure-verb issue I discussed above. I won't point out each of them, but this is an example of what I struggled with. I suggest instead something like "In Figure 2, we plot summary dataset scatterplots overlaid with dual-polarization relationship fits."

Yes, we have revised 'Figure * plot' examples throughout the text.

7.16 Suggest " . . . convective environments that favor enhanced evaporation, cooling and subsidence, which are less capable of sustaining . . . "

Accepted. Thanks.

7.28 why is "For" capitalized in "For example"?

OK. Changed that to "for example"

8.5 what is less influenced? What is the object of this clause?

Agree. Rephrased as, 'This reduced coefficient variability reflects on the closer relationship between A and K_{DP} with rainfall rate, less influenced by the presence/absence of select larger drop sizes.'

8.10 I'd suggest just saying "higher extreme parameter spaces" instead of saying "select" and then saying what it is anyhow.

Agree. Thanks.

8.30 suggest removing comma after "loosely"

Accepted. Thanks.

9.10 suggest "The results in Figure 6 . . ."

Agree. Thanks.

9.25 Suggest " . . . included modest convective diversity, including congestus clouds, and clouds with maritime, continental, and deeper convective properties (those supporting additional graupel growth)."

Accepted. Thanks.

9.27 suggest " . . . conditions than what is observed over the Amazon."

Accepted. Thanks.

9.31 suggest " . . . limitations for imposing BR concepts when characterizing . . ."

Agree. Thanks.

9.33 can you put "herein TM" within the parentheses?

Done. Thanks.

10.4 suggest "either" instead of "belonging to"

Accepted. Thanks.

10.14 suggest " . . . as is similar to . . ."

Agree. Thanks.

10.18 " . . . having corresponding stratiform DSDs (or, the absence thereof) . . ." seems contradictory. If having a corresponding stratiform DSD is indicative of TM oceanic characteristics, why then would also its absence?

Agree that this is awkward. Rephrased as, "In contrast, DSDs associated with ETH < 9 km carry DSD properties most similar to TM oceanic characteristics, having corresponding stratiform DSDs that favor smaller median drop sizing than deeper column counterparts."

10.22 you say "adjacent" and then describe "transitional" - are they the same? and if so, can you pick one?

Agree. Replaced 'adjacent' with 'Transitional'.

11.4 "a bright band signature"

Agree. Thanks.

11.18 suggest removing "are those that"

Agree. Thanks.

12.2 Suggest excising the sentence "A more practical . . . GoAmazon2014/5." it's awkward here.

Agree. Have removed this line.

12.14 the letters in "convective available potential energy" don't need to be capitalized.

Agree. Thanks.

12.16 suggest removing "that" from "studies that indicate"

Agree. Thanks.

13.1 suggest ". . . drops, and toward parameter spaces . . ."

Accepted. Thanks.

13.3 "though they do support"

Agree. Thanks.

13.4 perhaps change title to "Role of Pollution in Oceanic Signatures"?

Agree. Thanks.

13.12 suggest "The rightmost panels of Figure 15 show a composite mean . . ."

Accepted. Thanks.

13.16 remove ", respectively"

Accepted. Thanks.

13.17-23 Here is the paragraph in which I struggled with the presentation of representative statistics.

Yes. We can add a line to this paragraph that points to the supplemental material that contains histograms for the MUCAPE and MUCIN.

14.5 "One explanation . . . is that more prominent . . . contributions are acting within these convective columns . . ."

Agree. Thanks.

14.16 " . . . suggest that cleaner aerosol conditions are associated . . ."

Agree. Thanks.

14.31 suggest " . . . wind directions, and therefore should not be as influenced . . . "

Accepted. Thanks.

14.33 suggest "(e.g., local sources)"

Accepted. Thanks.

15.19 " . . . explanations for why these outliers cluster . . ."

Agree. Thanks.

15.29 suggest " . . .initiation and subsequent precipitation . . ."

Accepted. Thanks.

15.33 change "were" to "was"

Agree. Thanks.

15.35 suggest "tended to be associated"

Agree. Thanks.

16.11 suggest removing "properties"

Agree. Thanks.

16.16-onward - use caution with throwing the word "storm" around. You haven't defined what a storm is, and I'm guessing you don't mean a thunderstorm. You don't use this word until this last section. I'd suggest saying "event" from here onward, just to be safe.

OK. Agree. Thanks.

16.22 ". . . continental behaviors as seen in previous studies . . ."

Agree. Thanks.

16.26 swap "Consulting" with "Considering"

Agree. Thanks.

16.28 remove "radiosonde" - the balloons aren't doing the forcing (although that would be some wild micro-scale meteorology!)

Agree. Thanks.

16.29 suggest "character of the congestus"

Agree. Thanks.

16.30 suggest "segregating by wind direction"

Agree. Thanks.

17.3 "a topic of future consideration"

Agree. Thanks.

Track changes of "The Green Ocean: Precipitation Insights from the GoAmazon2014/5 Experiment"

Die Wang[1], Scott E. Giangrande[1], Mary Jane Bartholomew[1], Joseph Hardin[2], Zhe Feng[2], Ryan Thalman[3], and Luiz A. T. Machado[4]

[1]Environmental and Climate Sciences Department, Brookhaven National Laboratory, Upton, NY, USA
[2]Pacific Northwest National Laboratory, Richland, WA
[3]Department of Chemistry, Snow College, Richfield, UT, USA
[4]National Institute for Space Research, Sao Jose dos Campos, Brazil

Correspondence to: D. Wang (diewang@bnl.gov)

Abstract. This study summarizes the precipitation properties collected during the GoAmazon2014/5 campaign near Manaus in central Amazonia, Brazil. Precipitation breakdowns, summary radar rainfall relationships and self-consistency concepts from a coupled disdrometer and radar wind profiler measurements are presented. The properties of Amazon cumulus and associated stratiform precipitation are discussed, including segregations according to seasonal (Wet/Dry regime) variability, cloud echo-top height and possible aerosol influences on the apparent oceanic characteristics of the precipitation drop size distributions. Overall, we observe that the Amazon precipitation straddles behaviors found during previous U.S. Department of Energy Atmospheric Radiation Measurements program (ARM) tropical deployments, with distributions favoring higher concentrations of smaller drops than ARM continental examples. Oceanic type precipitation characteristics are predominantly observed during the Amazon Wet seasons. An exploration of the controls on Wet season precipitation properties reveals that wind direction, as compared with other standard radiosonde thermodynamic parameters or aerosol count/regime classifications performed at the ARM site, provides a good indicator for those Wet season Amazon events having an oceanic character for their precipitation drop size distributions.

1 Introduction

Global climate models (GCMs) continuously improve to overcome deficiencies in climate predictions associated with cloud and precipitation processes (e.g., Klein and Genio, 2006; Del Genio, 2012). Following suit, observational studies serve to ~~better~~ inform GCM and cloud resolving model (CRM) activities by providing the physical understanding for more diverse, climatically significant global cloud conditions and their associated feedbacks. Cumulus to deeper convective clouds are associated with high impact weather events and act as the engine of the global circulation. Subsequently, model treatments of convection have profound impact on weather and climate simulations. For practical reasons, the evaluation of cumulus treatments has often stressed comparisons against larger-scale, longer-term precipitation properties; for example, accumulated rainfall products from ground or space-borne instruments (e.g., Hou et al., 2014). ~~Thus, improving precipitation measurements (i.e., those that better reflect the natural variability of clouds under diverse forcing conditions) has traditionally supported improved convective treatments.~~ Thus, a traditional observational approach in support of convective modeling has been to document global precipitation variability and improve basic rainfall retrievals. Nevertheless, improving model capabilities ~~are introducing~~ introduces new challenges that motivate multi-scale, multi-sensor observations to better constrain cloud microphysics and dynamics closer to the process levels future GCMs attempt to represent (e.g., Mather and Voyles, 2013; Donner et al., 2016).

Recently, the Observations and Modeling of the Green Ocean Amazon (GoAmazon2014/5) Experiment was motivated by demands to gain a better understanding of aerosol, cloud and precipitation interactions on climate and the global circulation (Martin et al., 2016, 2017). ~~The inability of GCMs to adequately represent cumulus clouds and precipitation over the Amazon highlights one example of the observational needs for future improvement to GCM cloud parameterizations and the larger-scale circulation connections therein (Richter and Xie, 2008, Nobre et al., 2009, Yin et al., 2013. A low-level barrier when developing useful observational constraints is the shortage of long-term datasets for reference within tropical regions such as the Amazon basin. Geophysical retrievals of interest for precipitation studies include radar-based rainfall estimation, but even basic radar preprocessing improvements for dual-polarization quantities can be critical for future studies utilizing forward radar model comparisons.~~ One source of uncertainty when developing useful precipitation retrievals for model development is the shortage of long-term surface gauge and disdrometer observations within tropical regions. Although radar rainfall estimation and its uncertainty for tropical applications is of primary interest, basic radar preprocessing, calibration and dual-polarization radar data quality is also improved with extended surface precipitation records in diverse environments. Establishing boundaries for tropical ~~measurement~~ precipitation expectations and radar data quality concepts (e.g., Scarchilli et al., 1996, self-consistency methods) provides an immediate benefit when interpreting remote radar deployments including those from the Atmospheric Radiation Measurement (Ackerman and Stokes, 2003, ARM) Mobile Facility (Miller et al., 2016, AMF) during GoAmazon2014/5. Specifically, the Amazon basin offers a unique tropical perspective on the variability of precipitation, as it receives copious precipitation across diverse cloud conditions, including 'Wet' and 'Dry' seasonal variability interconnected to large-scale shifts in the thermodynamic forcing and coupled local cloud-scale feedbacks (e.g., Machado et al., 2004; Cifelli et al., 2004; Li and Fu, 2004; Misra, 2008).

~~Although anchoring hydrological retrievals is of a practical significance, an interesting scientific perspective from previous Amazon precipitation studies are those promoting the Amazon as a 'Green Ocean'. This terminology references the unique regional characteristics observed from the convection that spans oceanic to continental cloud extremes in key attributes such as updraft intensities and propensity for electrification.~~ Although improving hydrological retrievals is of a practical significance, an interesting outcome from previous Amazon studies is the labelling of the Amazon as the 'Green Ocean'. This Green Ocean terminology is rooted in studies such as Roberts et al. (2001) wherein low cloud condensation nuclei (CCN) concentrations and high CCN to condensation nuclei (CN) ratios over the Amazon resembled marine environments, as distinct from previous continental expectations. However, this terminology is often extended to include the unique regional characteristics observed from Amazon convection that spans oceanic to continental cloud extremes in key attributes such as updraft intensities and propensity for electrification. ~~Specifically~~ Specific to convection, Amazon clouds may initiate under these clean (or lower) ~~cloud condensation nuclei (~~CCN~~)~~ conditions, over a pristine forest, but also experience a range of thermodynamical and aerosol forcing influences that promote changes in cloud properties including electrification, cloud droplet size distribution and precipitation changes, or enhanced updraft intensity (e.g., Williams et al., 2002; Cecchini et al., 2016; Giangrande et al., 2016b, 2017). As described by Williams et al. (2002), the prevalence of maritime convective cloud regimes over a large continent are possibly still underappreciated in the convective spectrum and its intensity, especially given the propensity to identify deeper convection over the Amazon having electrification arguing continental convective characteristics.

To ~~better~~ understand the diversity of convective clouds as well as to constrain upcoming convective modeling activities from GoAmazon2014/5, it is informative to explore Amazon cumulus characteristics over this extended dataset. ~~One motivation is to question, "When is the Green Ocean 'blue'?", towards identifying conditions under which precipitation sampled in the Amazon basin adheres more towards oceanic, maritime to possible continental characteristics~~ One motivation for this study is to identify conditions under which precipitation sampled in the Amazon basin adheres more towards oceanic, maritime and continental characteristics. (e.g., Tokay and Short, 1996). Previous ARM Tropical Western Pacific (e.g., Long et al., 2016, TWP) precipitation studies have helped identify practical thresholds and composite behaviors for convection, as well as the strengths/deficiencies for more practical convective cloud regime segregations under various larger-scale monsoonal and more oceanic cloud environments (e.g., Bringi et al., 2003; Giangrande et al., 2014a; Thompson et al., 2015). ~~In addition to better addressing Amazon precipitation in the context of global variability, it is useful to assess whether traditional (or, practical) radar remote-sensing (including dual-polarization) quantities are sensitive to these shifts.~~ While it is important to view these Amazon datasets and cloud or larger-scale regime shifts in the context of global disdrometer observations (e.g., Dolan et al., 2018), it is also useful to determine whether common remote-sensing platforms (e.g., dual-polarization quantities as from X-band to S-band radars) are sensitive to these differences.

This study summarizes the precipitation properties collected by the ARM AMF during GoAmazon2014/5 at the 'T3' site located approximately 70 km to the west of Manaus in central Amazonia, Brazil ($3°12'46.70''$S, $60°35'53.0''$ W). The location samples both the local pristine atmosphere and possible effects of the Manaus, Brazil pollution plume. The T3 site was equipped to capture a continuous convective cloud and precipitation column characteristics from a reconfigured radar wind profiler coupled with a ground disdrometer. Section 2 describes the instrumentation, methods and sources for uncertainty in results presented by this study. Precipitation comparisons from the disdrometer using traditional drop size distribution (DSD) parameters and dual-polarization quantities ~~useful for future hydrological applications~~ are located in Section 3. Sections 4 and 5 discuss the properties of the Amazon cumulus convective and associated stratiform precipitation, including segregations according to seasonal (Wet/Dry regime) variability, cloud height and possible aerosol influences. A summary of the key findings and discussions about Amazon as a 'Green Ocean' are provided in the final section.

2 Dataset and Methodology

2.1 ~~The~~ ARM T3 Precipitation and Radar Wind Profiler Dataset and Processing

Precipitation observations are obtained from two primary instruments, a second-generation PARSIVEL disdrometer (e.g., Löffler-Mang and Joss, 2000; Tokay et al., 2014; Bartholomew, 2014) and a reconfigured 1290 MHz radar wind profiler (Giangrande et al., 2013, 2016b; Coulter et al., 2009, RWP). The collocated sensors capture surface DSDs, as well as simultaneous profiles for the vertical velocity and reflectivity factor estimates through the depth of Amazon clouds. These instruments operated concurrently from September 2014 through December 2015, ~~periods~~ a period that captured one 'Wet' season (herein, the five months defined as December through April) and one 'Dry' season (herein, periods from June through September). Additional information on the AMF deployment, including details on the larger-scale thermodynamic sampling throughout the campaign and appropriateness for Wet/Dry regime separations, is found in the GoAmazon2014/5 overview by Giangrande et al. (2017).

PARSIVEL measurements such as estimated DSD parameters and additional derived radar quantities are determined using 5-min aggregation windows. This sampling reduces noisiness found in 1-minute DSD quantity retrievals, which is reduced further by selecting 5-minute DSDs having $R > 0.5$ $\mathrm{mmhr^{-1}}$ and total drops > 100. In total, 3852 5-minute DSDs were collected during the GoAmazon2014/5 campaign, with 3087 associated with the collocated RWP observations. The total precipitation associated with the full set of DSD observations is 2597 mm, with 2511 mm associated with collocated RWP observations. Approximately 1500 mm were associated with convective precipitation (RWP classifications to be discussed in later sections). Processing for the disdrometer was performed using the open-source PyDSD code (Hardin, 2014), with standard corrections (e.g., Tokay et al., 2013, 2014). Estimated quantities include the rainfall rate R ($\mathrm{mmhr^{-1}}$), rain water content LWC ($\mathrm{gm^{-3}}$), measured median volume drop size D_0 (mm), the mass-weighted mean diameter D_m (mm). Processing also includes additional parameters of a gamma-fit DSD assumed of the form $N(D) = N_0 D^{\mu}\exp(-\Lambda D)$, having equivalent volume diameter D (mm) with number concentration N_0 ($\mathrm{mm^{-1}m^{-3}}$), shape parameter μ, and slope parameter Λ ($\mathrm{mm^{-1}}$) calculated following a method of higher moments (second, fourth, and sixth moment, e.g., Cao and Zhang (2009)).

Additional calculations for a normalized DSD intercept parameter N_w have been adapted following Testud et al. (2001). These are required to investigate a DSD-based convective-stratiform partitioning scheme based on disdrometer observations (e.g., Bringi et al., 2002, 2003, 2009). Dual-polarization radar quantities including the radar reflectivity factor Z (dBZ), differential reflectivity factor Z_{DR} (dB), specific differential phase K_{DP} ($\mathrm{degkm^{-1}}$) and specific attenuation A ($\mathrm{dBkm^{-1}}$, horizontal polarization) are estimated for liquid media at 20°C using a T-Matrix approach (e.g., Mishchenko et al., 1996). These estimates assume nonspherical drop shapes according to the relationship in Thurai et al. (2007) and standard drop canting assumptions for S-band (10-cm), C-band (5.45-cm) and X-band (3.16-cm) wavelengths.

RWP measurement details have been summarized by several recent studies, with precipitation datasets available at high spatiotemporal resolution of approximately 15 seconds and 200 meters (e.g., Tridon et al., 2013; Giangrande et al., 2013). To align with the 5-minute disdrometer measurements, an RWP profile from the mid-point of the 5-minute window are selected. RWP measurements are typically stable with respect to Z calibration offsets, with measurements aligned to those from the surface disdrometer (typically viable to within $2\ \mathrm{dB}$). Echo-top height (ETH) from the RWP is defined as the altitude where column Z drops below $10\ \mathrm{dBZ}$. Amazon RWP observations indicate this relative Z altitude as the approximate height that mean convective cloud vertical velocity approaches $0\ \mathrm{ms}^{-1}$. Vertical air velocity retrievals and echo classifications follow techniques outlined by Giangrande et al. (2016b). For echo classifications, ~~we first identify higher confidence convective and stratiform regions on the basis of column Z signatures and/or so-called radar 'bright band' (melting-level) designations for longer wavelengths~~ we identify convective and stratiform regions on the basis of column Z signatures, velocity properties, and/or so-called radar 'bright band' (melting-level) designations for longer wavelengths (e.g., Fabry and Zawadzki, 1995; Williams et al., 1995; Geerts and Dawei 2004). In contrast to scanning radar-based echo designations (e.g., those typically use near surface $Z \simeq$ 40-45 dBZ thresholds, e.g., Steiner et al. (1995)), one RWP advantage is that columns exhibiting stronger vertical air velocity signatures help to further differentiate transitional or elevated convective cells (e.g., instances of $|VV| > 2\ \mathrm{ms}^{-1}$).

2.2 ~~The~~ ARM T3 Aerosol Observations and Aerosol Regime Classification

Aerosol regime classifications are based on the combination of number concentration of particles ~~condensation nuclei (~~CN~~)~~, measurements for the fraction of particles with diameters less than $70\ \mathrm{nm}$, and carbon monoxide CO and oxides of Nitrogen (NO_y) measurements at the T3 location using instrumentation as described in Thalman et al. (2017) and supplemental materials. The philosophy for this aerosol classification is that each aerosol measurement builds on the previous when establishing a background condition ('clean'), with additional support for 'polluted' conditions (e.g., urban, above this background condition) as well as 'biomass' burning conditions attributed on top of 'polluted' criteria. One advantage for using this classification is that this combination of measurements helps mitigate concerns that precipitation onset will mask ambient aerosol conditions (e.g., as in including an insoluble CO measurement). Because of the pronounced shift in aerosol properties seasonally, the methods sub-classify background and polluted air mass types according to seasonal-specific windows. Classifications are available at 5-minute intervals that align with the available precipitation observations.

As summarized by Thalman et al. (2017), 'clean' conditions (typical background levels) exhibit values CN < $500\ \mathrm{cm}^{-3}$, CO < $0.14\ \mathrm{ppm}$ and NO_y < $1.5\ \mathrm{ppbv}$ during the Wet season. In contrast, background levels ~~and associated classifications~~ shift towards values of CN $\simeq 1500\ \mathrm{cm}^{-3}$ (e.g., potentially factor of 3 or more difference in CN) for similar CO and NO_y thresholds during the Dry season (Transitional months fall between Wet/Dry characteristics). In this regard, the Dry season background conditions reflect regional biomass burning background levels that might otherwise be considered polluted conditions during typical Wet season months. For this study, sampling limitations during the GoAmazon2014/5 Dry season (lack of available collocated precipitation and aerosol measurements) requires our use of only Wet season observations to provide a more detailed aerosol-cloud-precipitation investigation. Under Wet season conditions, 'polluted' regimes are those having CN > $500\ \mathrm{cm}^{-3}$. 'Biomass' regimes are considered a more stringent polluted classification, classified as those 'polluted' regimes also having CO > $0.14\ \mathrm{ppm}$.

2.3 PARSIVEL Sampling and Rainfall Relationship Interpretation

Later sections document relationships between estimated radar quantities and the measured rainfall rate R. These quantities carry instrument sampling considerations that include catchment uncertainties under convective conditions (e.g., Duchon and Essenberg, 2001), additional limitations when compared to collocated devices (e.g., Tokay et al., 2013; Park et al., 2017; Thurai et al., 2017), and/or processing assumptions when applying functional-form DSD parameter fits (e.g., Smith et al., 2009; Cao and Zhang, 2009). Radar quantities as estimated by disdrometer are also influenced by raindrop shape and additional assumptions introducing variability established in previous studies (e.g., Thurai et al., 2007). Given our comparisons between rainfall accumulations with surface gauge measurements under typical storm intensities, as well as previous side-by-side performance testing of other PARSIVEL units, we do not anticipate ~~estimated~~ radar quantity uncertainty falling outside the variability established by previous studies. However, reasonable instrument offsets for radar quantities such as Z may be on the order of 10-20 % or 1-2 dBZ.

An additional consideration when fitting rainfall relationships is the representativeness of this dataset, including challenges when attempting to establish the significance of functional fits. We establish coefficients for conventional $R(Z)$ relationships of the form $Z = aR^b$ using nonlinear least squares methods matched over the entire dataset (or subsets) of Z-R pairs. For lengthier datasets, it is informative to test variability in coefficients as related to modest samples drawn from the total population. Since consecutive DSD observations within precipitation events are non-independent and correlated in processes (e.g., Lee et al., 2009), it may be important to consider this impact of proper spacing between samples when ensuring a reliable relationship.

~~Figure 1 plots~~ As plotted in Figure 1, we show histograms for ~~'a'-coefficient~~ a-coefficient values from various single parameter rainfall relationships (radar quantities estimated as in previous sections), assuming a fixed ~~'b'-coefficient~~ b-coefficient as determined from our complete Amazon dataset for the S-band wavelength. This example highlights the sensitivity in the ~~'a'-coefficients~~ a-coefficients as estimated from random half-dataset subsets to the complete dataset (vertical black line). Assuming a constant b-coefficient $\simeq$ 1.4 is typically a reasonable assumption to assist in microphysical interpretation from $R(Z)$ relationships for size-controlled conditions (e.g., Steiner et al., 2004). As the radar wavelength decreases, the sampling sensitivity depends on the radar quantity of interest. For example, the differences we observe for Amazon subsamples are typically to within 5 % of the mean dataset ~~'a'-coefficient~~ a-coefficient value with respect to $R(Z)$. ~~A deterioration to~~ Though not shown in Figure 1, a deterioration in performance at shorter wavelengths is found for $R(Z)$ relationships owing to the importance of larger diameters to Z estimates and increased non-Rayleigh scattering. In contrast, ~~'a'-coefficients~~ a-coefficients are found typically to within 2 % for $R(K_{DP})$ and $R(A)$ relations, with improved performance to shorter wavelengths (more immediate relationship between these quantities and rainfall rate). ~~Such results help inform basic interpretations for the significant changes in these radar relationship coefficients.~~ Such results help inform basic interpretations of the significant changes (larger than that expected from subsampling) in these radar relationship coefficients. The corresponding plots for C-band and X-band are provided in the supplemental materials (Figures S1 and S2).

3 Summary Precipitation Results and Interpretation for Retrieval Methods

This section summarizes bulk precipitation properties, rainfall relationships, and basic dual-polarization radar connections for the GoAmazon2014/5 dataset. A summary of DSD parameter breakdowns for select quantities, filtered according to rainfall rate intervals, is located in Table 1. As one point of comparison to continental expectations, we include values obtained from a year-long ARM Southern Great Plains (SGP) PARSIVEL2 deployment (November 2016 through October 2017), processed similar to the Amazon datasets. Within these narrowed rainfall rate intervals, the Amazon precipitation exhibits reduced median drop sizes and higher drop concentrations. This change is also reflected in lower Z values and higher LWC for a similar R as compared to SGP observations. Although the 5-minute Dry season samples are limited, rainfall rate breakdowns demonstrate the Dry season exhibits ~~higher-relative~~ higher relative Z and median drop sizes (lower N_w and LWC) as compared to Wet season observations. Discrepancies between SGP and Amazon, as well as Wet/Dry separations, are most pronounced at the higher R consistent with convective cores. This is likely based on the propensity for observing melting hail in deeper SGP convection and/or larger observing melting aggregates in stratiform regions trailing convective lines. Both SGP situations would favor sampling larger drop sizes at the surface.

3.1 Single-parameter Dual-polarization Rainfall Relationships at S- C- and X-band

~~Figure 2 plots~~ In Figure 2, we plot summary dataset scatterplots and overlaid dual-polarization relationship fits for the S-band wavelength. The corresponding plots for C- and X-band are provided in the supplemental materials (Figures S3 and S4). A summary of matched rainfall coefficients is provided in Table 2. For these tables, ~~'b'-coefficients~~ b-coefficients were fixed at a characteristic dataset value to facilitate comparison across regime breakdowns. ~~Figure 2 overlays~~ In Figure 2, we overlay the associated fitting (dashed lines) from SGP-Oklahoma to provide a continental reference. As a function of radar wavelength, the 'a'-coefficient values decrease as wavelength decreases (e.g., quantities more closely related to the rainfall rate). SGP dual-polarization relationships are consistent with previous studies (e.g., Giangrande et al., 2014b), providing confidence in the appropriateness of disdrometer processing. Note, minor discrepancies in SGP $R(Z)$ relations may be related to our filtering of large drops > 5 mm that disproportionately influence Z measurements at sites including SGP wherein melting hail is more regularly observable. Moreover, SGP relations may carry higher ~~'a'-coefficients~~ a-coefficients (thus, larger discrepancies with the Amazon relationships) than reported in our Table 2.

Summary Amazon relationships follow a tropical expectation (more significant role for warm-rain processes, e.g., droplet growth via collision-coalescence), indicating higher concentrations of smaller drops. This is observed when having a smaller ~~'a'-coefficient~~ a-coefficient than found for SGP $R(Z)$ relations, and larger ~~'a'-coefficients~~ a-coefficients than found for SGP $R(K_{DP})$ and $R(A)$ relations (as in Figure 2). These changes reflect a significant change when viewed compared to Amazon dataset sampling arguments found in Section 2. For Table 2, $R(A)$ relationships are also listed for multiple temperature assumptions, highlighting one explanation for modest variability when attempting to promote these relations for practical rainfall retrievals (e.g., Ryzhkov et al., 2014; Giangrande et al., 2014b). As additional reference for dual-polarization radar processing and natural calibration concepts, self-consistency relationships between radar quantities K_{DP}, Z, and Z_{DR} for the various wavelengths have been provided in Table 2. In comparison to continental SGP references for statistical DSD relationships (e.g., Ryzhkov et al., 2005), self-consistency coefficients in Table 2 reinforce the tropical character of the Amazon precipitation, again consistent with smaller median drop sizing (e.g., reductions in Z_{DR} or K_{DP}) to achieve similar estimates of Z.

Rainfall relationships stratified according to Wet and Dry season conditions are also found in Table 2. The Wet season indicates lower ~~'a'-coefficients~~ a-coefficients for $R(Z)$ and higher relative coefficients for $R(K_{DP})$ and $R(A)$ relations. One interpretation is that for similar R, the Wet season DSDs carry the more pronounced tropical precipitation characteristics. A similar trend is found with seasonal self-consistency relationship breakdowns. As before, most seasonal breakdowns are reflected as significant changes in relationship coefficients when compared the sampling arguments in Section 2. An exception to this are K_{DP}-based rainfall relationships that appear least sensitive to this seasonal DSD variability at X-band (the shortest wavelength tested), possibly a reflection of non-Rayleigh influences on K_{DP} (i.e., the presence/absence of larger drops) is less important.

Finally, interpreting seasonal differences can be challenging without mentioning factors including storm intensity changes related to the larger-scale thermodynamic shifts that alter convective and congestus frequency, or mid-level moisture (e.g., during GoAmazon2014/5 as in Giangrande et al. (2017), cf. 2). ~~The Dry season promotes storms that achieve higher rainfall rate R, but under convective environments favoring enhanced evaporation, cooling and subsidence less capable to sustain expansive stratiform processes.~~ The Dry season promotes events that achieve higher rainfall rate R, but under convective environments that favor enhanced evaporation, cooling and subsidence, which are less capable of sustaining expansive stratiform processes. Wet and ~~adjacent transitional~~ Transitional month stratiform precipitation linked to aggregation and associated DSD evolution processes beneath the melting layer favors lower N_w, higher D_0 values for similar Z (e.g., Giangrande et al., 2016a). The fraction of stratiform DSDs (count) to the total DSD observations in this dataset for the Wet season is 50.5 %. This fraction decreases to approximately 30.1 % for the Dry season. ~~Nevertheless, summary rainfall accumulations/properties skew heavily towards convective designations for all seasons, as reported in Table 3 and discussed further in Section 4.~~ Nevertheless, summary rainfall properties skew heavily towards convective designations for all seasons, as reported in Table S1. Seasonal changes will be discussed further in Section 4 in the context of multiparameter DSD breakdowns.

3.2 Convective/Stratiform Regimes for Rainfall Relationships and DSD Properties

Isolating contributions from convective and stratiform DSDs is an initial step for improved rainfall estimates or possible model evaluation (e.g., Tokay and Short, 1996). Table 2 is segregated according to RWP-based convective/stratiform echo classifications. These RWP-based segregations will be further decomposed in Section 4, but for demonstration purposes are considered a reasonable benchmark when isolating bulk regime contributions. Cumulative contoured frequency altitude display histograms (e.g., Yuter and Houze, 1995, CFADs) with quantile values (median, 90th and 95th percentile) for RWP Z and vertical velocity retrieval profiles are plotted in Figure 3. These histograms help establish these RWP classifications as reasonable; For example, convective columns (Figures 3a and 3c) have monotonically decreasing profiles and stronger vertical motions, whereas stratiform (Figure 3b, 3d) columns emphasize pronounced radar 'bright band' - or, aggregation process signatures and weaker composite upwards vertical air velocity signatures (e.g., Fabry and Zawadzki, 1995). Given that checks for pronounced 'bright band' signatures are part of the echo classification, that these signatures are observed is not surprising. Inflation of mid-level downwards motions in stratiform regions is observed near the freezing level, originating from contamination within the melting layer on fall speed corrections (e.g., enhanced Z from aggregation resulting in overestimates for ice fall speeds).

In terms of rainfall relationships in Table 2, convective relationships demonstrate higher coefficient values for $R(K_{DP})$ relations and smaller coefficients for $R(Z)$ relations. This shift is consistent with convection favoring high N_w, low D_0 for a similar Z or K_{DP}. $R(A)$ relationships register as those least influenced by these separations (smallest coefficient shifts), followed by K_{DP} relationships at the shorter wavelengths. This ~~performance~~ reduced coefficient variability reflects on the closer relationship between A and K_{DP} with rainfall rate, less influenced by the presence/absence of select larger drop sizes. As complementary examples for the Amazon datasets, Figure 4 plots the corresponding histograms for Amazon convective and stratiform DSDs in terms of N_w (Figure 4a), LWC versus R relationships (Figure 4b), and D_0 variations with Z (Figure 4c). For these plots, convection is noted by red shadings and stratiform is plotted in blue contours. Convection demonstrates a broader distribution of N_w, LWC and other quantities of interest. Although there is substantial overlap with stratiform DSDs, convective DSDs exclusively cover ~~select (higher extreme)~~ higher extreme parameter spaces.

4 Amazon Precipitation Properties: Cumulative Dataset Characteristics

Convection-permitting models struggle to simultaneously capture convective and stratiform cloud processes, therefore model-observational comparisons often emphasize bulk cloud regime segregations and contingent performances to diagnose issues with cloud model treatments (e.g., Lang et al., 2003). Although there is no clear line separating convective and stratiform processes (e.g., for identifying deficiencies in modeled precipitation, vertical air motions or heating profiles), bulk regime separations introduced for Section 3 are of practical use. Here, we assess how precipitation depictions from previous campaigns might be useful to constrain Amazon observations and the sensitivity of radar quantities to those changes.

Precipitating clouds identified by the RWP demonstrate a clear bimodal ETH distribution (Figure 5), and one that varies according to Amazon seasons (Figure 5a). The behaviors are consistent with freezing level (typically, around 5 km above surface) and tropopause-level cloud-top expectations for tropical convection (Figure 5b, e.g., Johnson et al. (1999); Jensen and Del Genio (2006)). Note also that the RWP is not sensitive to cloud-sized particles, thus actual cloud top heights (as from collocated cloud radar referenecs) may extend 2 km or more above these heights. Sounding-based winds over the T3 site are predominantly easterly (mostly observed during the Dry season) to northeasterly (mostly, Wet season) (Figure 5c), with low-level Z observations (Figure 5d) illustrating that Amazon cumulus are often linked to relatively modest values of $Z \simeq 35$ dBZ. From a practical radar-based classification perspective that typically utilizes higher $Z \simeq$ 40-45 dBZ thresholds, it follows that standard methods may necessitate additional texture, peakedness or similar ideas to properly identify Amazon convection (e.g., Steiner et al., 1995).

As documented by Giangrande et al. (2017, cf. 6 and 8), convection passing over T3 follows a diurnal cycle with peak cloud frequency around local 13-14 h. A shift in peak frequency to the later afternoon is found within the Dry season, whereas

Wet season deeper convection exhibits a secondary peak in cloud frequency (related to mesoscale convective systems) during the overnight hours. Congestus clouds (loosely, precipitating clouds having ETHs between 4.5 km and 9 km) demonstrate a similar diurnal pattern across all Amazon seasons. The frequency of all precipitating clouds (congestus and deeper) increases substantially for the Amazon Wet season. Of additional note, the precipitation originating from congestus or possible shallower forms of tropical organized cloud systems (as defined solely on RWP-based ETH < 9 km in Chen and Liu (2015)) is nontrivial for this Amazon dataset (accumulations as reported in Table ~~3~~ S1.

~~Figure 6 plots~~ As plotted in Figure 6, we show the frequency for observing various levels of vertical air motions ~~(magnitude exceeding threshold as on Figure 6)~~ within an RWP column as additional reference to the convective character of these clouds. Displays present these frequencies as a function of a lower-level RWP Z ($\simeq 2$ km). To lower ranges of Z (< 35 dBZ), we observe a stable percentage of columns having vertical air motions around $1\ \mathrm{ms}^{-1}$. This may be viewable as also the baseline uncertainty regarding RWP-based vertical velocity retrievals. As Z increases above 35 dBZ, we observe a rapid increase in the frequency of stronger updrafts/downdrafts, indicative of the increasing contributions from convective clouds sharing these relative Z levels. As Z is stronger, the likelihood of sampling deeper clouds (and therefore additional chance to observe a stronger velocity in those column) also will increase as a function of Z. Results in Figure 6 also provide some guidance in convective/stratiform classification methods for scanning radars that use low-level Z thresholds (e.g., Steiner et al., 1995). Specifically, low-level Z exceeding a 40 dBZ value (or higher) is a reasonable designation of convection in absence of vertical velocity measurements.

4.1 Disdrometer Convective-Stratiform Segregation: Alignment with RWP Signatures

~~Figure 7 plots~~ In Figure 7, a convective-stratiform regime segregation concept is shown, with the solid line as reference to a DSD-based classification in following Bringi et al. (2003)~~,~~ (herein BR). In this N_w versus D_0 space, BR proposed that tropical maritime convective precipitation observed at Darwin, Australia falls to the right of the solid black line in Figure 7. In terms of thresholds, for this dataset the DSDs best aligned with falling on either side of the BR line correspond to those having a rainfall rate threshold of $13\ \mathrm{mmhr}^{-1}$, or a Z value of 40 dBZ. ~~Figure 7 also overlays~~ In Figure 7, we also overlay the contours the RWP-based classifications for convective (red colors) and stratiform (blue lines) precipitating columns. The ellipse on Figure 7 indicates the two-sigma confidence interval for those regions containing stratiform DSDs as based on the RWP classification.

RWP-based classifications indicate that substantial DSDs may be attributed to convective classifications left of this BR line. These are associated with the RWP identifying congestus or shallower convective cloud columns, as based on velocity signatures. However, the Amazon dataset supports bulk BR findings for deeper tropical convection in that precipitation to the right of the BR line is exclusive to convective designations. Since BR was developed using a Darwin monsoonal dataset, we anticipate that study included modest convective diversity ~~into congestus clouds, maritime continental~~ , including congestus clouds, and clouds with maritime, continental, and deeper convective properties (those supporting additional graupel growth). Darwin may exhibit even more intense 'Break' (e.g., more continental characteristics) convective cell periods and associated DSD changes interspersed with maritime tropical 'Active' monsoonal conditions than ~~observed from Amazon convection~~ what is observed over the Amazon (e.g., May and Ballinger, 2007; Dolan et al., 2013; Schumacher et al., 2015; Giangrande et al., 2014a, 2016b). However, it appears use of BR would minimize the contributions from congestus or shallower organized convective precipitation found under Amazon conditions.

More recently, Thompson et al. (2015) highlighted limitations for imposing BR concepts ~~if~~ when characterizing oceanic precipitation observed over ARM Tropical Western Pacific (TWP) ground disdrometers at Manus island and Equatorial Indian Ocean Gan islands. Thompson et al. (2015)~~,~~ (herein TM), proposed a unique oceanic convective-stratiform segregation having origins in LWC and D_0 space. One justification for this change was to ~~better~~ isolate DSD clusters exhibiting the higher concentrations of smaller drops consistent with oceanic-convective clouds favoring warm-rain processes/collision-coalescence over mixed-phase and/or stratiform particle growth. The TM classification is simple to implement, since it overlaps within the BR space as a line of constant $\log10(N_w) \simeq 3.85\ \mathrm{m^{-3}mm^{-1}}$. ~~Figure 8 orients this dataset in BR/TM formulation spaces to the left of the BR line, with the DSDs identified as belonging to convective or stratiform (based on the RWP definitions) noted on the panels.~~ As plotted in Figure 8, we consider only the DSDs that would fall to the left of the BR separation line (e.g., those that follow a traditional BR stratiform designation). For this figure, the DSDs identified as belonging to convective or stratiform (based on the RWP definitions) are then subset according to the left and right panels, respectively. When populations from the Amazon DSDs exhibit more oceanic qualities (residing above the dashed TM line), contributions to the histograms (Figures 8a, 8c) are typically associated with RWP convection signatures. Similarly, DSDs identified as stratiform by the RWP (Figures 8b, 8d) follow those residing below the TM criteria for oceanic-like stratiform precipitation. Overall, bulk Amazon precipitation carries several hybrid characteristics as found from previous ARM tropical DSD studies.

4.2 Cumulative Precipitation Properties According to Cloud Regime and Season

Extending the previous analysis into cloud regimes, ~~Figure 9 separates~~ in Figure 9 we separate Amazon precipitation according to ETH values above/below 9 km. This choice follows the discussion from Figure 5 and is assumed as a reasonable proxy to also help separate statistical congestus from deeper convective events. These plots include combined convective precipitation (e.g., stronger updraft/downdraft regions) as well as associated trailing stratiform DSDs and/or decaying convection.

~~Figure 9 indicates that~~ As shown in Figure 9, deeper cumulus clouds are associated with additional maritime continental DSD properties as is similar to Darwin studies, with fewer observations residing above TM recommendations for possible oceanic characteristics. Deeper convective and stratiform DSDs as designated by the RWP exhibit more frequent DSD examples having larger median drop sizes. In contrast, DSDs associated with ETH < 9 km carry DSD properties most similar to TM oceanic characteristics, having corresponding stratiform DSDs ~~(or, the absence thereof)~~ that ~~also~~ favor smaller median drop sizing than deeper column counterparts. While tempting to attribute these oceanic ETH < 9 km DSD characteristics solely to weak, isolated congestus clouds, inspection of the events reveals oceanic DSDs are often associated with widespread convective lines and/or widespread convective cells (to be further discussed).

Figure 10 illustrates this cloud segregation according to Dry, Wet and ~~adjacent~~ Transitional months (here, ’Transitional’ implying May, October and November properties that share qualities of both Wet/Dry seasons). The Dry season conditions (Figures 10a, 10d) skew towards bulk precipitation properties associated with the deeper convective clouds from above. These properties follow an isolated, stronger convective cell expectation for Dry season precipitation, that also includes an absence of

DSDs associated with detrained stratiform precipitation processes (e.g., low N_w, larger D_0) as to be discussed in the following section. In contrast, Wet season DSD characteristics (Figures 10b, 10e) follow previous tropical and oceanic expectations, with additional excursions into DSD contributions associated with the convective core modes (right of BR).

4.3 Stratiform Precipitation Properties Associated with Amazon Convective Events

Stratiform precipitation within the Amazon is commonly observed during the Wet season and ~~adjacent~~ Transitional months, associated with the detrained regions from deeper convective cells or cell dissipation. Increased stratiform precipitation frequency during the Wet season is attributed to factors including the seasonal change in midlevel moisture and reductions in Wet season convective inhibition more supportive of convective initiation and prevalence. Recalling Figures 8b and 8d, stratiform DSDs as identified by the RWP often are the same as combining thoughts from BR/TM recommendations. This statement is further confirmed consulting cumulative and fractional convective precipitation as in Table ~~3~~ S1. ~~Figure 11 presents~~ In Figure 11, we present the composite DSD properties as reported in Figure 9, exclusive to RWP-indicated stratiform properties. Contours overlaid on Figure 11 indicate those DSD regions designated as having a ~~bright-band~~ bright band signatures in the column. As from the left panels in Figure 11 (ETH > 9 km), locations with profiles exhibiting clear bright band signatures correspond well with BR expectations for stratiform precipitation; ~~F~~ for example, these would often represent the DSDs within more developed precipitation trailing deeper convective cells, mesoscale convective systems (e.g., Houze, 1997).

Lower echo-top stratiform characteristics (ETH < 9 km) indicate two unique clusters. The first cluster represents observations associated with aggregation processes that produce stronger melting layer signals, similar to ETH > 9 km examples. These observations are found under Wet season conditions (50 $\%$ of the available DSDs), and are less common under Dry season conditions (30 $\%$ of the available DSDs). Initially, this supports an argument that enhanced Wet season moisture influences sustained stratiform development, ice growth (deposition), and eventual aggregation processes. The second cluster is associated with smaller median drop sizes and higher-relative number concentrations. This represents the more prevalent stratiform mode for lower-top Dry season observations, and is equally frequent for Wet season observations. This cluster argues for less developed stratiform processes, either owing to the lack of mid-level moisture in Dry season profiles, or consistent with Wet season widespread, weaker congestus (e.g., reduced inhibition resulting in larger areas having weaker updraft intensity).

4.4 Implications of Convective-Stratiform Partitioning

Previous sections indicate that RWP and hybrid BR/TM classifications ~~are those that~~ faithfully differentiate congestus and deeper convective DSDs from stratiform DSDs. Table ~~3~~ S1 reports the total convective precipitation and fractional convective precipitation for this GoAmazon2014/5 dataset. These values are estimated according to segregations from BR methods, a hybrid BR/TM combination, the RWP classification, and a simple rainfall rate $R > 10\ \mathrm{mm hr^{-1}}$ threshold. Table ~~3~~ S1 has also been segregated according to Wet/Dry and Transitional season component behaviors.

For the Amazon dataset, both TM/BR and RWP methods attribute approximately half of the total precipitation (convective plus stratiform) to possible congestus or shallower cloud regimes, as defined by our ETH < 9 km definitions. Moreover, we observe that the fractional convective precipitation is higher for those methods adding additional complexity to the classification.

Convective fractions suggest differences to within $\simeq 10$ %. Seasonal breakdowns confirm that the Wet season and ~~adjacent~~ Transitional months are more dominated by stratiform rainfall, with transitional months suggesting the largest share of stratiform precipitation. Overall, fractional convective contributions are high (exceeding 80%), but the strong agreement between RWP and BR/TM ideas gives confidence that traditional radar segregations would report lower convective fractions owing to incorrect attribution of congestus or shallower-topped precipitation systems.

It is possible to check whether dual-polarization radar quantities are sensitive to apparent variations between congestus, deeper convection and associated stratiform precipitation properties. Figure 12 plots (Z, Z_{DR}) scatterplot as well as a (K_{DP}-Z-Z_{DR}) self-consistency curve behaviors for various regimes identified by the RWP; ~~L~~ lower panels in Figure 12 illustrate the Wet and Dry season segregations. For all panels in Figure 12, we present X-band dual-polarization estimates calculated from T-Matrix scattering, as radar quantities at these shorter wavelengths should be more sensitive to lower rainfall rate conditions. ~~A more practical consideration for these ideas is to support future studies from a dual-polarization X-band radar that was operated during GoAmazon2014/5.~~ The radar quantities are presented in terms of their associated two-sigma confidence regions (ellipses). Since radars routinely perform separate ETH and/or bright-band designation checks, the demonstrations in Figure 12 are not a true reference for what is possible from a robust radar echo classification methodology. However, Figure 12 suggests substantial overlap between these cloud precipitation regimes when placed in this dual-polarization context. This would suggest X-band or longer-wavelength radars would not be sufficient constraints for regime classifications without additional information. The most pronounced contrasts are those observed between Wet/Dry seasons, wherein the Dry season favors the larger extremes for all dual-polarization radar quantities, associated with the contributions of larger drops.

5 Amazon Precipitation Properties: The Green Ocean Characteristics

The Amazon Wet season has been highlighted for its copious precipitation owing to factors including enhanced moisture and reduced convective inhibition (CIN). One additional consideration is that these conditions, possibly when coupled with cleaner atmospheric aerosol profiles, may promote the so-called 'Green Ocean' or oceanic cloud and precipitation characteristics. In contrast, Dry season convective conditions migrate towards enhanced Convective Available Potential Energy (CAPE) and stronger CIN that may promote stronger convective ~~storms~~ events, initiating within more polluted atmospheric states closer to continental regimes. Other recent Amazon studies ~~that~~ indicate that the convection that initiates during the Amazon Dry season exhibits more intense vertical air motions and precipitation properties (e.g., Giangrande et al., 2016b; Schiro, 2017).

5.1 The Amazon 'Green Ocean': When Do We Observe Oceanic Behaviors?

~~Figure 13 extends~~ As shown in Figure 13, we extend the previous analysis found in Figure 10 to a seasonal comparison between deeper clouds (ETH > 9 km, reds) and congestus or shallower convection (ETH < 9 km, blues). To simplify, 'stratiform' DSD components (as identified by the RWP) have been removed from this figure. Although all DSDs are assumed as 'convective', it is instructive to focus on DSDs in Figure 13 located to the right of the BR separation line, as those DSDs correspond to the most confident convective conditions having typical rainfall rate $R > 13\ \mathrm{mm hr^{-1}}$. As also in Table 1, convective Dry season DSDs carry fewer drops, but larger median drop sizes. Physically, this corresponds well with expectations that stronger updrafts in the Dry season should promote larger droplet sizes as a consequence of mixed-phase growth. Wet season characteristics are noticeably shifted towards higher number concentrations, with lower-relative LWC. This is consistent with the anticipated changes towards more oceanic and/or tropical warm-rain processes, cleaner and/or weaker updraft ~~storms~~ events. For dual-polarization radar studies, these characteristics are consistent with Dry season convection exhibiting larger values in Z_{DR} or K_{DP} for a similar value of Z, noting surface conditions may also be modified slightly from the conditions sampled aloft from radar.

~~Figure 14 plots~~ We show, in Figure 14, congestus and deep convective full DSD averages for convective conditions as in Figure 13. Average DSDs are also provided for those observations found to the right of the BR separation line, as well as those DSDs having $Z > 35$ dBZ. Overall, composite behaviors emphasize that Dry season convective precipitation (and into convective core regions) is skewed towards an increased presence of larger drops, and toward parameter spaces favoring higher LWC for a similar D_0. In contrast to Wet season properties, Amazon Dry season precipitation conditions are not consistent with TM oceanic findings (shift towards DSDs having increased larger drops), though they do support that the updrafts in the Dry season are stronger.

5.2 The Amazon 'Green Ocean': Role of Pollution on Oceanic Signatures?

Overall, the primary shift in precipitation properties for the Amazon coincides with changes in the larger-scale seasonal shifts in thermodynamics and aerosol conditions. In this respect, it is difficult to differentiate relative controls, especially given sampling limits of our Amazon precipitation dataset during the Dry season. However, the frequent Wet season convective instances (removing the more obvious stratiform contributions) offers some opportunity to test whether we observe any sensitivity to background aerosol conditions and/or other environmental conditions when promoting so-called oceanic DSD properties.

~~Figure 15 plots~~ As plotted in Figure 15, we show the set of convective DSDs observed during the Wet season, identifying the relative clean (blues) and polluted (reds) aerosol conditions. Panels beneath the cumulative convective plots illustrate the convective DSDs associated with column ETH < 9 km. ~~Rightmost panels on Figure 15 plot~~ The rightmost panels of Figure 15 show a composite median, 90th and 95th percentile RWP Z profile under the clean and polluted conditions, respectively. For simplicity, polluted regimes in our study combine the more stringent (but, in this dataset, the more frequent) 'biomass' polluted classification with standard 'polluted' designations. During this campaign, a total of 82 clean and 61 polluted events were collected having at least one 5-minute convective DSD, with 66 clean events registering an ETH < 9 km DSD and 46 polluted events with a ETH < 9 km DSD~~, respectively~~.

The mean thermodynamic conditions are sampled from the morning 12 UTC radiosondes. For this dataset, clean events record a mean (standard deviation) most unstable MUCAPE of 2124 (1100) $\mathrm{Jkg^{-1}K^{-1}}$, most unstable MUCIN of -34 (42) $\mathrm{Jkg^{-1}K^{-1}}$, and average 0-5 km RH of 83 (6) $\%$. Polluted events are slightly more favorable to deeper convection, in recording a higher mean MUCAPE of 2567 (1176) $\mathrm{Jkg^{-1}K^{-1}}$, with an MUCIN of -35 (36) $\mathrm{Jkg^{-1}K^{-1}}$ and RH of 80 (7) $\%$, respectively. Histograms of MUCAPE and MUCIN are shown in the supplemental materials (Figure S5). Both clean and polluted events share a similar mean freezing level height at approximately 4.8 km. Overall, it is still important to suggest the polluted cases should be more conducive to deeper events based on the available dataset. For the ETH < 9 km panels, mean clean (polluted) environments appear less favorable, with MUCAPE of 1993 (2388) $\mathrm{Jkg^{-1}K^{-1}}$, MUCIN of -36 (-38) $\mathrm{Jkg^{-1}K^{-1}}$, and RH of 83 (81) $\%$. Standard deviations for clean (polluted) values are similar as ETH > 9 km convection.

Figure 15 indicates that cleaner regime convective precipitation during the Wet season agrees well with oceanic expectations as reported by TM and discussions above. Cumulative polluted regime convective results are less consistent with oceanic expectations, but there is overlap emphasizing DSDs associated with ETH < 9 km columns. Deeper ETH > 9 km polluted convective observations (deeper convection properties) are those most skewed towards Dry season and/or least oceanic behaviors, including hints of stratiform-type DSD excursions. Inevitably, some DSD contamination could follow from convective-to-stratiform transitional columns in the strongest storms as well, for example those featuring sloped updrafts having stronger vertical motions aloft overhanging a stratiform-type downdraft in the column below

Bulk clean/polluted contrasts are potentially visible on the composite Z profiles, with cleaner regime composites demonstrating an increasing Z profile (Z weighted towards increasing contributions from larger drops) towards the surface. One explanation is that these cleaner profiles more routinely are associated with collisional growth process contributions influencing Z profiles over evaporation and/or breakup process influences on radar signatures (e.g., evaporation and/or breakup acting to reduce Z, perhaps not observable with available larger drops to RWP wavelengths). These profile behaviors are pronounced for the ETH < 9 km observations that should minimize mixed-phase process influences. In contrast, the polluted regime profiles indicate similar and/or larger Z values aloft to approximately 3.0 km AGL, with Z profiles peaking and/or decrease in magnitude below these altitudes.

One explanation for the polluted profile characteristics in Figure 15 ~~are~~ is that more prominent mixed-phase particle process contributions are acting within these convective columns. Since these polluted events demonstrate more favorable mean thermodynamic conditions that favor stronger convective updrafts, it is possible that an updraft enhancement partially elicits such a transition. A similar response may also be attributed to the proposed role of aerosols in following invigoration arguments (e.g., Rosenfeld et al., 2008). For example, recent Amazon aircraft studies as in Braga et al. (2017) indicate changes such as an absence of liquid within growing convective cumulus during polluted conditions, and/or differences in the relative formation/altitudes of ice particles. Regardless of process path, the suggestion is that polluted convective columns would be those that potentially promote added ice depositional growth (resulting in fewer, but larger ice particles at the expense of additional liquid). Such physical arguments could help explain the similar or larger Z magnitude aloft (larger ice sizing, offsetting density), coupled with a modest melting enhancement followed by a reduction in Z below 5 km. A reduced number of particles under this scenario would also reduce collisional growth below the freezing level as compared to the cleaner profiles. Overall, surface DSD properties in Figure 15 suggest ~~cleaner aerosol~~ that cleaner aerosol conditions as associated with enhanced oceanic DSD properties (aka, in agreement with select 'Green Ocean' statements). However, it is nonobvious whether these lesser oceanic conditions (esp. within the deeper cores having fewer samples) were the consequence of the aerosol conditions, or the shift in the environmental conditions that tracked the change in aerosol.

5.3 The Amazon 'Green Ocean': An Alternate Explanation

It is useful to determine whether we can better deconvolve environmental influences from aerosol as those more important to the prevalence of oceanic precipitation characteristics. ~~Figure 16 plots~~ In Figure 16, we show Wet season DSDs contingent on the ambient wind directions, with relative breakdowns according to the northeasterly/east-southeasterly (NE/ESE) and east/east-northeast (E/ENE) directional pairings. First, the specific (NE/ESE) and (E/ENE) pairings were selected for having similar DSD sample sizes. Second, these wind orientations may also be viewed as relevant with respect to the Manaus pollution plume (e.g., E and ENE flows over T3 as arguably the more polluted relative to the Manaus location).

~~Figure 16 highlights~~ In Figure 16, we highlight evidence of oceanic-type DSD behaviors according to most wind directions. The fractional 'polluted' versus 'clean' DSD breakdowns along these directions are as follows: NE: 57 % clean 43 % polluted; ENE: 68 % clean 32 % polluted; E: 94 % clean 6 % polluted; ESE: 91 % clean 9 % polluted. Following Figure 16, it is found that the larger DSD outlier populations (e.g., convective DSDs found to be least 'oceanic' when compared with TM) are observed for NE and ESE wind directions ~~that~~ , and therefore should not be as influenced by possible Manaus pollution plume. Note, most polluted events sampled during the Wet season were attributed to 'biomass' classifications, e.g., local aerosol sources, which may explain NE flows as those most polluted. As expected from discussions above, slightly stronger 12 UTC MUCAPE (STD) values are also found along the NE and ENE directions (2207 (1325) $\mathrm{Jkg^{-1}K^{-1}}$ and 2131 (934) $\mathrm{Jkg^{-1}K^{-1}}$, respectively) that are associated with bulk polluted events, while the weakest potential forcing conditions are found with the ESE and E flows (2089 (1241) $\mathrm{Jkg^{-1}K^{-1}}$ and 1766 (1035) $\mathrm{Jkg^{-1}K^{-1}}$, respectively). Nevertheless, these local thermodynamic controls associated with wind direction are far less pronounced than previous polluted/clean contrasts. The histograms for MUCAPE and MUCIN as a function of wind direction are found in the supplemental materials (Figure S6).

The DSDs observed along NE wind flows reflect the least oceanic characteristics in this dataset, favoring low N_w-D_0 pairings typical of Dry season convection (also carrying similar Z profiles as to Figure 15, not shown). Again, these NE flows reflect the most polluted wind components, and directions associated with the larger mean convective forcing parameters associated with higher values towards the tail of the MUCAPE distributions (Figure S6). In that regard, a reduced presence for oceanic-type DSDs was not unexpected. However, the pronounced absence of oceanic DSD characteristics along NE flows is far more noteworthy than when contrasted to previous clean/polluted criteria, and not immediately in line with ~~local~~ mean thermodynamic ~~changes~~ values. From event inspection, most nonoceanic DSD characteristics were associated with isolated, deeper convective cell events, or widespread convective events still demonstrating deeper cloud ETH. Widespread, shallower convective events or organized shallow systems (possible Amazon warm-rain dominant systems as observed over oceans, e.g., Chen and Liu (2015)) were not favored, as compared with other wind components. Again, this change may be attributed to the frequency of higher MUCAPE at the tail of the NE distribution (Figure 6S).

Additional outlier DSD populations (including several events having numerous oceanic DSD properties) are observed according to ESE wind directions (relatively clean). These DSDs reflect the presence of deeper convective DSDs (to the right of the BR separation line) that exhibit high concentrations of larger-relative drop sizes. These regions, although not typical of TM oceanic examples, are also not consistent with Amazon Dry season characteristics (having relatively higher triplet of LWC, D_0

and N_w). As in NE flow examples, the basic radiosonde parameter checks and aerosol forcing controls associated with these events are in-line with the other wind components. However, histograms in Figure S6 do show a similar enhancement for the frequency of higher MUCAPE values towards the tail of the distribution.

As far as potential explanations for these outliers to cluster according to particular wind directions as compared to other environmental factors, it is important to note that while Amazon convection timing follows a well-established diurnal cycle over T3, 12 UTC radiosondes and associated parameters (those typically closest to earlier convective initiation) may not be completely representative of the important larger-scale conditions (e.g., South Atlantic Convergence Zone (SACZ) positioning, influences into the Amazon basin during the Wet season, Carvalho et al. (2004)). For one example, Wet season sea-breeze intrusion and associated statistical cloud enhancements (as determined by satellite) into the Amazon basin orient tangential to a NE-SW axis over the T3. This sea-breeze front passage is in phase with this T3 diurnal precipitation cycle (e.g., see composite convective evolution as in Burleyson et al. (2016)). It is possible that similar forms of dynamical or moisture enhancements, for example SACZ drivers of frontal intrusions, as well as river breeze influences (e.g., Tanaka et al., 2014; Burleyson et al., 2016), would not be completely captured by our morning radiosonde observations (given their timing). However, these larger-scale features may promote enhancements sufficient to spark possible changes in cloud initiation, subsequent precipitation properties.

From inspection of events according to wind directions, ESE events tended to emphasize widespread organized convective events exhibiting copious rainfall along a NE-SW orientation (with winds flowing from ESE preceding those lines), having shallower ETH < 9 km. Timing for these events were near or just following the afternoon diurnal maximum (18-20 UTC). One suggestion is that the oceanic DSDs tended to be those associated with these shallower, but widespread convective events initiated or enhanced by sea-breeze , Kelvin wave, or other influences. As the conditions are also clean, this is also consistent with shallower, oceanic forms of organized convection. These combined concepts and possible SACZ influences on these events are the subject of ongoing research. In contrast, NE events most often reflected deeper events (ETH > 9 km) with less evidence for forms of NE-SW linear or shallow cloud organization for animations of the widespread events. Deeper clouds would be consistent with pollution arguments as above, but these breakdowns speak to the complexities of these studies.

6 Conclusions

This study summarizes Amazon precipitation properties collected during the unique, multi-year GoAmazon2014/5 campaign. Emphasis was placed on cumulative campaign precipitation properties and relationships that may benefit potential hydrological applications and radar-based precipitation data product development, as well as connections relevant to future Amazon convective model evaluation. The study also explored Amazon precipitation properties from the perspective of possible ’Green Ocean’ convective characteristics, including possible thermodynamic and aerosol forcing influences that may be influential to observations of oceanic-like precipitation properties.

Amazon rainfall and radar self-consistency relationships demonstrate tropical characteristics as compared to continental SGP references, associated with radar quantities (in both convective and stratiform contexts) that sample higher relative concentrations of smaller drops. Typically, this indicates a reduced role for convective mixed-phase and/or graupel growth, as well as stratiform aggregation processes in the Amazon. These tropical precipitation characteristics are more pronounced within the Wet seasons than Dry season events, with Dry season storms favoring the presence of larger drop sizes as a suggested consequence of stronger storm updrafts under more favorable thermodynamic conditions. Although it is difficult to differentiate Wet/Dry regimes exclusively using radar quantities, our analysis suggests Z, Z_{DR} and K_{DP} would exhibit larger values within Dry season events and deeper convective cores therein.

Coupled RWP and disdrometer Amazon T3 precipitation breakdowns confirm the overall findings of previous ARM campaign BR and TM studies on tropical convective to oceanic type cloud and precipitation breakdowns. Amazon precipitation is varied and often found to straddle maritime continental behaviors of previous studies, with DSD excursions into the more oceanic examples presented from ARM Manus/Gan deployments. As before, the separations between Wet and Dry seasons are pronounced, with most oceanic DSD conditions observed during the Wet season. The strongest convective behaviors, as well as storms having a marked absence of stratiform precipitation, are observed during Amazon Dry season.

~~Consulting~~ Considering deeper versus congestus properties, Amazon congestus are attributed to the more oceanic precipitation behaviors found in our dataset. When exploring 'Green Ocean' themes, our analysis was not able to demonstrate that either aerosol conditions or enhanced local ~~radiosonde~~ convective forcing parameters were strongly associated with the presence/absence of an oceanic character to the congestus and deeper precipitation. Rather, the more pronounced separation was found when segregating ~~on~~ by wind direction, which may reflect that our initial options for thermodynamic or aerosol controls are all unable to deconvolve a more subtle change important to an enhanced DSD signature. However, there is evidence to support that aerosol or other early morning forcing factors within the Wet season are not significantly different to promote these differences. Rather, episodic to frequent Amazon basin larger-scale (e.g., SACZ, sea-breeze) or river forcing controls and associated enhancements may require future investigation to determine their importance to the apparent oceanic nature of the clouds and eventual precipitation. Other factors including the possible role of aerosol sizing (e.g., Fan et al., 2018) on updraft and precipitation enhancements for Amazon convection are also the topic of future consideration.

Data availability. All ARM datasets used for this study can be downloaded at http://www.arm.gov and associated with several "value added product" streams.

Competing interests. The authors declare that they have no conflict of interest.

Acknowledgements. This paper has been authored by employees of Brookhaven Science Associates, LLC, under contract no. DE-SC0012704 with the U.S. Department of Energy (DOE). The publisher by accepting the paper for publication acknowledges that the United States Government retains a non-exclusive, paid-up, irrevocable, world-wide license to publish or reproduce the published form of this paper, or allow others to do so, for United States Government purposes. Dr. Joseph Hardin and Dr. Zhe Feng at the Pacific Northwest National Laboratory (PNNL) are supported by the Climate Model Development and Validation activity funded by the Office of Biological and Environmental Research in the U.S. Department of Energy Office of Science also acknowledge the Atmospheric Radiation Measurement (ARM) Climate Research Facility, a user facility of the U.S. DOE, Office of Science, sponsored by the Office of Biological and Environmental Research, and support from the ASR program of that office.

References

Ackerman, T. P. and Stokes, G. M.: The Atmospheric Radiation Measurement Program, Phys. Today, 56, 38–44, https://doi.org/10.1063/1.1554135, 2003.

Bartholomew, M.: ARM's Handbook for the Parsivel2 Laser Disdrometer., Tech. rep., U.S. DOE, Office of Science, Office of Biological and Environmental Research, 2014.

Braga, R. C., Rosenfeld, D., Weigel, R., Jurkat, T., Andreae, M. O., Wendisch, M., Pöschl, U., Voigt, C., Mahnke, C., Borrmann, S., Albrecht, R. I., Molleker, S., Vila, D. A., Machado, L. A. T., and Grulich, L.: Further evidence for CCN aerosol concentrations determining the height of warm rain and ice initiation in convective clouds over the Amazon basin, Atmospheric Chemistry and Physics, 17, 14 433–14 456, https://doi.org/10.5194/acp-17-14433-2017, https://www.atmos-chem-phys.net/17/14433/2017/, 2017.

Bringi, V. N., Huang, G.-J., Chandrasekar, V., and Gorgucci, E.: A Methodology for Estimating the Parameters of a Gamma Raindrop Size Distribution Model from Polarimetric Radar Data: Application to a Squall-Line Event from the TRMM/Brazil Campaign, Journal of Atmospheric and Oceanic Technology, 19, 633–645, https://doi.org/10.1175/1520-0426(2002)019<0633:AMFETP>2.0.CO;2, https://doi.org/10.1175/1520-0426(2002)019<0633:AMFETP>2.0.CO;2, 2002.

Bringi, V. N., Chandrasekar, V., Hubbert, J., Gorgucci, E., Randeu, W. L., and Schoenhuber, M.: Raindrop Size Distribution in Different Climatic Regimes from Disdrometer and Dual-Polarized Radar Analysis, Journal of the Atmospheric Sciences, 60, 354–365, https://doi.org/10.1175/1520-0469(2003)060<0354:RSDIDC>2.0.CO;2, https://doi.org/10.1175/1520-0469(2003)060<0354:RSDIDC>2.0.CO;2, 2003.

Bringi, V. N., Williams, C. R., Thurai, M., and May, P. T.: Using Dual-Polarized Radar and Dual-Frequency Profiler for DSD Characterization: A Case Study from Darwin, Australia, Journal of Atmospheric and Oceanic Technology, 26, 2107–2122, https://doi.org/10.1175/2009JTECHA1258.1, https://doi.org/10.1175/2009JTECHA1258.1, 2009.

Burleyson, C. D., Feng, Z., Hagos, S. M., Fast, J., Machado, L. A. T., and Martin, S. T.: Spatial Variability of the Background Diurnal Cycle of Deep Convection around the GoAmazon2014/5 Field Campaign Sites, Journal of Applied Meteorology and Climatology, 55, 1579–1598, https://doi.org/10.1175/JAMC-D-15-0229.1, https://doi.org/10.1175/JAMC-D-15-0229.1, 2016.

Cao, Q. and Zhang, G.: Errors in Estimating Raindrop Size Distribution Parameters Employing Disdrometer and Simulated Raindrop Spectra, Journal of Applied Meteorology and Climatology, 48, 406–425, https://doi.org/10.1175/2008JAMC2026.1, https://doi.org/10.1175/2008JAMC2026.1, 2009.

Carvalho, L. M. V., Jones, C., and Liebmann, B.: The South Atlantic Convergence Zone: Intensity, Form, Persistence, and Relationships with Intraseasonal to Interannual Activity and Extreme Rainfall., Journal of Climate, 17, 88–108, 2004.

Cecchini, M. A., Machado, L. A. T., Comstock, J. M., Mei, F., Wang, J., Fan, J., Tomlinson, J. M., Schmid, B., Albrecht, R., Martin, S. T., and Artaxo, P.: Impacts of the Manaus pollution plume on the microphysical properties of Amazonian warm-phase clouds in the wet season, Atmospheric Chemistry and Physics, 16, 7029–7041, https://doi.org/10.5194/acp-16-7029-2016, https://www.atmos-chem-phys.net/16/7029/2016/, 2016.

Chen, B. and Liu, C.: Warm organized rain systems over the topical eastern Pacific, Journal of Climate, 29, 151009125047 002, 2015.

Cifelli, R., Carey, L., Petersen, W. A., and Rutledge, S. A.: An Ensemble Study of Wet Season Convection in Southwest Amazonia: Kinematics and Implications for Diabatic Heating, Journal of Climate, 17, 4692–4707, https://doi.org/10.1175/JCLI-3236.1, https://doi.org/10.1175/JCLI-3236.1, 2004.

Coulter, R., Martin, T., and Muradyan, P.: Updated hourly, Radar Wind Profiler (1290RWPPRECIPMOM)., Tech. rep., Atmospheric Radiation Measurement (ARM) Climate Research Facility Data Archive: Oak Ridge, Tenn., 2009.

Del Genio, A. D.: Representing the Sensitivity of Convective Cloud Systems to Tropospheric Humidity in General Circulation Models, Surveys in Geophysics, 33, 637–656, https://doi.org/10.1007/s10712-011-9148-9, https://doi.org/10.1007/s10712-011-9148-9, 2012.

Dolan, B., Rutledge, S. A., Lim, S., Chandrasekar, V., and Thurai, M.: A Robust C-Band Hydrometeor Identification Algorithm and Application to a Long-Term Polarimetric Radar Dataset, Journal of Applied Meteorology and Climatology, 52, 2162–2186, https://doi.org/10.1175/JAMC-D-12-0275.1, https://doi.org/10.1175/JAMC-D-12-0275.1, 2013.

Dolan, B., Fuchs, B., Rutledge, S. A., Barnes, E. A., and Thompson, E. J.: Primary Modes of Global Drop Size Distributions, Journal of the Atmospheric Sciences, 75, 1453–1476, https://doi.org/10.1175/JAS-D-17-0242.1, 2018.

Donner, L. J., O'Brien, T. A., Rieger, D., Vogel, B., and Cooke, W. F.: Are atmospheric updrafts a key to unlocking climate forcing and sensitivity?, Atmospheric Chemistry and Physics, 16, 12 983–12 992, https://doi.org/10.5194/acp-16-12983-2016, https://www.atmos-chem-phys.net/16/12983/2016/, 2016.

Duchon, C. E. and Essenberg, G. R.: Comparative rainfall observations from pit and aboveground rain gauges with and without wind shields, Water Resour. Res., 37, 3253?3263, https://doi.org/10.1029/2001WR000541, 2001.

Fabry, F. and Zawadzki, I.: Long-Term Radar Observations of the Melting Layer of Precipitation and Their Interpretation, Journal of the Atmospheric Sciences, 52, 838–851, https://doi.org/10.1175/1520-0469(1995)052<0838:LTROOT>2.0.CO;2, 1995.

Fan, J., Rosenfeld, D., Zhang, Y., Giangrande, S. E., Li, Z., Machado, L. A. T., Martin, S. T., Yang, Y., Wang, J., Artaxo, P., Barbosa, H. M. J., Braga, R. C., Comstock, J. M., Feng, Z., Gao, W., Gomes, H. B., Mei, F., Pöhlker, C., Pöhlker, M. L., Pöschl, U., and de Souza, R. A. F.: Substantial convection and precipitation enhancements by ultrafine aerosol particles, Science, 359, 411–418, https://doi.org/10.1126/science.aan8461, http://science.sciencemag.org/content/359/6374/411, 2018.

Geerts, B. and Dawei, Y.: Classification and Characterization of Tropical Precipitation Based on High-Resolution Airborne Vertical Incidence Radar. Part I: Classification, Journal of Applied Meteorology (1988-2005), 43, 1554–1566, http://www.jstor.org/stable/26186013, 2004.

Giangrande, S. E., Collis, S., Straka, J., Protat, A., Williams, C., and Krueger, S.: A Summary of Convective-Core Vertical Velocity Properties Using ARM UHF Wind Profilers in Oklahoma, Journal of Applied Meteorology and Climatology, 52, 2278–2295, https://doi.org/10.1175/JAMC-D-12-0185.1, https://doi.org/10.1175/JAMC-D-12-0185.1, 2013.

Giangrande, S. E., Bartholomew, M. J., Pope, M., Collis, S., and Jensen, M. P.: A Summary of Precipitation Characteristics from the 2006–11 Northern Australian Wet Seasons as Revealed by ARM Disdrometer Research Facilities (Darwin, Australia), Journal of Applied Meteorology and Climatology, 53, 1213–1231, https://doi.org/10.1175/JAMC-D-13-0222.1, https://doi.org/10.1175/JAMC-D-13-0222.1, 2014a.

Giangrande, S. E., Collis, S., Theisen, A. K., and Tokay, A.: Precipitation Estimation from the ARM Distributed Radar Network during the MC3E Campaign, Journal of Applied Meteorology and Climatology, 53, 2130–2147, https://doi.org/10.1175/JAMC-D-13-0321.1, https://doi.org/10.1175/JAMC-D-13-0321.1, 2014b.

Giangrande, S. E., Toto, T., Bansemer, A., Kumjian, M. R., Mishra, S., and Ryzhkov, A. V.: Insights into riming and aggregation processes as revealed by aircraft, radar, and disdrometer observations for a 27 April 2011 widespread precipitation event, J. Geophys. Res. Atmos., 121, 5846?5863, https://doi.org/10.1002/2015JD024537, 2016a.

Giangrande, S. E., Toto, T., Jensen, M. P., Bartholomew, M. J., Feng, Z., Protat, A., Williams, C. R., Schumacher, C., and L.Machado: Convective cloud vertical velocity and mass-flux characteristics from radar wind profiler observations during GoAmazon2014/5, J. Geophys. Res. Atmos., 121, 12 891–12 913, https://doi.org/10.1002/2016JD025303, 2016b.

Giangrande, S. E., Feng, Z., Jensen, M. P., Comstock, J. M., Johnson, K. L., Toto, T., Wang, M., Burleyson, C., Bharadwaj, N., Mei, F., Machado, L. A. T., Manzi, A. O., Xie, S., Tang, S., Silva Dias, M. A. F., de Souza, R. A. F., Schumacher, C., and Martin, S. T.: Cloud characteristics, thermodynamic controls and radiative impacts during the Observations and Modeling of the Green Ocean Amazon (GoAmazon2014/5) experiment, Atmospheric Chemistry and Physics, 17, 14 519–14 541, https://doi.org/10.5194/acp-17-14519-2017, https://www.atmos-chem-phys.net/17/14519/2017/, 2017.

Hardin, J.: PyDisdrometer Version v1.0, 2014.

Hou, A. Y., Kakar, R. K., Neeck, S., Azarbarzin, A. A., Kummerow, C. D., Kojima, M., Oki, R., Nakamura, K., and Iguchi, T.: The Global Precipitation Measurement Mission, Bulletin of the American Meteorological Society, 95, 701–722, https://doi.org/10.1175/BAMS-D-13-00164.1, https://doi.org/10.1175/BAMS-D-13-00164.1, 2014.

Houze, R. A.: Stratiform Precipitation in Regions of Convection: A Meteorological Paradox?, Bulletin of the American Meteorological Society, 78, 2179–2196, https://doi.org/10.1175/1520-0477(1997)078<2179:SPIROC>2.0.CO;2, 1997.

Jensen, M. P. and Del Genio, A. D.: Factors Limiting Convective Cloud-Top Height at the ARM Nauru Island Climate Research Facility, Journal of Climate, 19, 2105–2117, https://doi.org/10.1175/JCLI3722.1, https://doi.org/10.1175/JCLI3722.1, 2006.

Johnson, R. H., Rickenbach, T. M., Rutledge, S. A., Ciesielski, P. E., and Schubert, W. H.: Trimodal Characteristics of Tropical Convection, Journal of Climate, 12, 2397–2418, https://doi.org/10.1175/1520-0442(1999)012<2397:TCOTC>2.0.CO;2, https://doi.org/10.1175/1520-0442(1999)012<2397:TCOTC>2.0.CO;2, 1999.

Klein, S. and Genio, A. D.: ARM's Support for GCM Improvement: A White Paper, Tech. rep., U.S. Department of Energy, Washington, D.C., 2006.

Lang, S., Tao, W.-K., Simpson, J., and Ferrier, B.: Modeling of Convective–Stratiform Precipitation Processes: Sensitivity to Partitioning Methods, Journal of Applied Meteorology, 42, 505–527, https://doi.org/10.1175/1520-0450(2003)042<0505:MOCSPP>2.0.CO;2, https://doi.org/10.1175/1520-0450(2003)042<0505:MOCSPP>2.0.CO;2, 2003.

Lee, C. K., Lee, G. W., Zawadzki, I., and Kim, K.-E.: A Preliminary Analysis of Spatial Variability of Raindrop Size Distributions during Stratiform Rain Events, Journal of Applied Meteorology and Climatology, 48, 270–283, https://doi.org/10.1175/2008JAMC1877.1, https://doi.org/10.1175/2008JAMC1877.1, 2009.

Li, W. and Fu, R.: Transition of the Large-Scale Atmospheric and Land Surface Conditions from the Dry to the Wet Season over Amazonia as Diagnosed by the ECMWF Re-Analysis, Journal of Climate, 17, 2637–2651, https://doi.org/10.1175/1520-0442(2004)017<2637:TOTLAA>2.0.CO;2, https://doi.org/10.1175/1520-0442(2004)017<2637:TOTLAA>2.0.CO;2, 2004.

Löffler-Mang, M. and Joss, J.: An Optical Disdrometer for Measuring Size and Velocity of Hydrometeors, Journal of Atmospheric and Oceanic Technology, 17, 130–139, https://doi.org/10.1175/1520-0426(2000)017<0130:AODFMS>2.0.CO;2, https://doi.org/10.1175/1520-0426(2000)017<0130:AODFMS>2.0.CO;2, 2000.

Long, C. N., Mather, J. H., and Ackerman, T. P.: The ARM Tropical Western Pacific (TWP) Sites, Meteorological Monographs, 57, 7.1–7.14, https://doi.org/10.1175/AMSMONOGRAPHS-D-15-0024.1, https://doi.org/10.1175/AMSMONOGRAPHS-D-15-0024.1, 2016.

Machado, L. A. T., Laurent, H., Dessay, N., and Miranda, I.: Seasonal and diurnal variability of convection over the Amazonia: A comparison of different vegetation types and large scale forcing, Theoretical and Applied Climatology, 78, 61–77, https://doi.org/10.1007/s00704-004-0044-9, https://doi.org/10.1007/s00704-004-0044-9, 2004.

Martin, S. T., Artaxo, P., Machado, L. A. T., Manzi, A. O., Souza, R. A. F., Schumacher, C., Wang, J., Andreae, M. O., Barbosa, H. M. J., Fan, J., Fisch, G., Goldstein, A. H., Guenther, A., Jimenez, J. L., Pöschl, U., Silva Dias, M. A., Smith, J. N., and Wendisch, M.: Introduction:

Observations and Modeling of the Green Ocean Amazon (GoAmazon2014/5), Atmospheric Chemistry and Physics, 16, 4785–4797, https://doi.org/10.5194/acp-16-4785-2016, https://www.atmos-chem-phys.net/16/4785/2016/, 2016.

Martin, S. T., Artaxo, P., Machado, L., Manzi, A. O., Souza, R. A. F., Schumacher, C., Wang, J., Biscaro, T., Brito, J., Calheiros, A., Jardine, K., Medeiros, A., Portela, B., de Sá, S. S., Adachi, K., Aiken, A. C., Albrecht, R., Alexander, L., Andreae, M. O., Barbosa, H. M. J., Buseck, P., Chand, D., Comstock, J. M., Day, D. A., Dubey, M., Fan, J., Fast, J., Fisch, G., Fortner, E., Giangrande, S., Gilles, M., Goldstein, A. H., Guenther, A., Hubbe, J., Jensen, M., Jimenez, J. L., Keutsch, F. N., Kim, S., Kuang, C., Laskin, A., McKinney, K., Mei, F., Miller, M., Nascimento, R., Pauliquevis, T., Pekour, M., Peres, J., Petäjä, T., Pöhlker, C., Pöschl, U., Rizzo, L., Schmid, B., Shilling, J. E., Dias, M. A. S., Smith, J. N., Tomlinson, J. M., Tóta, J., and Wendisch, M.: The Green Ocean Amazon Experiment (GoAmazon2014/5) Observes Pollution Affecting Gases, Aerosols, Clouds, and Rainfall over the Rain Forest, Bulletin of the American Meteorological Society, 98, 981–997, https://doi.org/10.1175/BAMS-D-15-00221.1, https://doi.org/10.1175/BAMS-D-15-00221.1, 2017.

Mather, J. H. and Voyles, J. W.: The Arm Climate Research Facility: A Review of Structure and Capabilities, Bulletin of the American Meteorological Society, 94, 377–392, https://doi.org/10.1175/BAMS-D-11-00218.1, https://doi.org/10.1175/BAMS-D-11-00218.1, 2013.

May, P. T. and Ballinger, A.: The Statistical Characteristics of Convective Cells in a Monsoon Regime (Darwin, Northern Australia), Monthly Weather Review, 135, 82–92, https://doi.org/10.1175/MWR3273.1, https://doi.org/10.1175/MWR3273.1, 2007.

Miller, M. A., Nitschke, K., Ackerman, T. P., Ferrell, W., Hickmon, N., and Ivey, M.: The Atmospheric Radiation Measurement Mobile Facility, The Atmospheric Radiation Measurement (ARM) Program: AMS Monograph, The first 20 years of ARM, Am. Meteorol. Soc., https://doi.org/10.1175/AMSMONOGRAPHS-D-15-0051.1, 2016.

Mishchenko, M., Travis, L., and Mackowski, D.: T-matrix computations of light scattering by nonspherical particles: A review, J. Quant. Spectrosc. Radiat. Transfer, 55, 535–575, https://doi.org/10.1016/0022-4073(96)00002-7, 1996.

Misra, V.: Coupled Air, Sea, and Land Interactions of the South American Monsoon, Journal of Climate, 21, 6389–6403, https://doi.org/10.1175/2008JCLI2497.1, https://doi.org/10.1175/2008JCLI2497.1, 2008.

Park, S.-G., Kim, H.-L., Ham, Y.-W., and Jung, S.-H.: Comparative Evaluation of the OTT PARSIVEL2 Using a Collocated Two-Dimensional Video Disdrometer, Journal of Atmospheric and Oceanic Technology, 34, 2059–2082, https://doi.org/10.1175/JTECH-D-16-0256.1, https://doi.org/10.1175/JTECH-D-16-0256.1, 2017.

Roberts, G. C., O., A. M., Jingchuan, Z., and Paulo, A.: Cloud condensation nuclei in the Amazon Basin: “marine” conditions over a continent?, Geophysical Research Letters, 28, 2807–2810, https://doi.org/10.1029/2000GL012585, 2001.

Rosenfeld, D., Lohmann, U., Raga, G. B., O’Dowd, C. D., Kulmala, M., Fuzzi, S., Reissell, A., and Andreae, M. O.: Flood or Drought: How Do Aerosols Affect Precipitation?, Science, 321, 1309–1313, https://doi.org/10.1126/science.1160606, http://science.sciencemag.org/content/321/5894/1309, 2008.

Ryzhkov, A., Diederich, M., Zhang, P., and Simmer, C.: Potential Utilization of Specific Attenuation for Rainfall Estimation, Mitigation of Partial Beam Blockage, and Radar Networking, Journal of Atmospheric and Oceanic Technology, 31, 599–619, https://doi.org/10.1175/JTECH-D-13-00038.1, https://doi.org/10.1175/JTECH-D-13-00038.1, 2014.

Ryzhkov, A. V., Giangrande, S. E., Melnikov, V. M., and Schuur, T. J.: Calibration Issues of Dual-Polarization Radar Measurements, Journal of Atmospheric and Oceanic Technology, 22, 1138–1155, https://doi.org/10.1175/JTECH1772.1, https://doi.org/10.1175/JTECH1772.1, 2005.

Scarchilli, G., Gorgucci, E., Chandrasekar, V., and Dobaie, A.: Self-consistency of polarization diversity measurement of rainfall, IEEE Trans. Geosci. Remote Sens., 34, 22–26, 1996.

Schiro, K. A.: Thermodynamic Controls on Deep Convection in the Tropics: Observations and Applications to Modeling, dissertation, University of California, 2017.

Schumacher, C., Stevenson, S. N., and Williams, C. R.: Vertical motions of the tropical convective cloud spectrum over Darwin, Australia., Q.J.R. Meteorol. Soc., 141, 2277–2288, 2015.

Smith, P. L., Kliche, D. V., and Johnson, R. W.: The Bias and Error in Moment Estimators for Parameters of Drop Size Distribution Functions: Sampling from Gamma Distributions, Journal of Applied Meteorology and Climatology, 48, 2118–2126, https://doi.org/10.1175/2009JAMC2114.1, https://doi.org/10.1175/2009JAMC2114.1, 2009.

Steiner, M., R. A. Houze, J., and Yuter, S. E.: Climatological characterization of three-dimensional storm structure from operational radar and rain gauge data, J. Appl. Meteorol., 34, 1978?2007, 1995.

Tanaka, L. M. d. S., Satyamurty, P., and Machado, L. A. T.: Diurnalcvariation of precipitation in central Amazon basin, Int J. Climatol., 34, 3574?3584, 2014.

Testud, J., Oury, S., Black, R. A., Amayenc, P., and Dou, X.: The Concept of "Normalized" Distribution to Describe Raindrop Spectra: A Tool for Cloud Physics and Cloud Remote Sensing, Journal of Applied Meteorology, 40, 1118–1140, https://doi.org/10.1175/1520-0450(2001)040<1118:TCONDT>2.0.CO;2, https://doi.org/10.1175/1520-0450(2001)040<1118:TCONDT>2.0.CO;2, 2001.

Thalman, R., de Sá, S. S., Palm, B. B., Barbosa, H. M. J., Pöhlker, M. L., Alexander, M. L., Brito, J., Carbone, S., Castillo, P., Day, D. A., Kuang, C., Manzi, A., Ng, N. L., Sedlacek III, A. J., Souza, R., Springston, S., Watson, T., Pöhlker, C., Pöschl, U., Andreae, M. O., Artaxo, P., Jimenez, J. L., Martin, S. T., and Wang, J.: CCN activity and organic hygroscopicity of aerosols downwind of an urban region in central Amazonia: seasonal and diel variations and impact of anthropogenic emissions, Atmospheric Chemistry and Physics, 17, 11 779–11 801, https://doi.org/10.5194/acp-17-11779-2017, https://www.atmos-chem-phys.net/17/11779/2017/, 2017.

Thompson, E. J., Rutledge, S. A., Dolan, B., and Thurai, M.: Drop Size Distributions and Radar Observations of Convective and Stratiform Rain over the Equatorial Indian and West Pacific Oceans, Journal of the Atmospheric Sciences, 72, 4091–4125, https://doi.org/10.1175/JAS-D-14-0206.1, https://doi.org/10.1175/JAS-D-14-0206.1, 2015.

Thurai, M., Huang, G. J., Bringi, V. N., Randeu, W. L., and Schönhuber, M.: Drop Shapes, Model Comparisons, and Calculations of Polarimetric Radar Parameters in Rain, Journal of Atmospheric and Oceanic Technology, 24, 1019–1032, https://doi.org/10.1175/JTECH2051.1, https://doi.org/10.1175/JTECH2051.1, 2007.

Thurai, M., Gatlin, P., Bringi, V. N., Petersen, W., Kennedy, P., Notaros, B., and Carey, L.: Toward completing the raindrops size spectrum: Case studies involving 2D-video disdrometer, droplet spectrometer, and polarimetric radar measurements, J. Appl. Meteor. Climatol., 56, 877?896, 2017.

Tokay, A. and Short, D. A.: Evidence from Tropical Raindrop Spectra of the Origin of Rain from Stratiform versus Convective Clouds, Journal of Applied Meteorology, 35, 355–371, https://doi.org/10.1175/1520-0450(1996)035<0355:EFTRSO>2.0.CO;2, https://doi.org/10.1175/1520-0450(1996)035<0355:EFTRSO>2.0.CO;2, 1996.

Tokay, A., Petersen, W. A., Gatlin, P., and Wingo, M.: Comparison of Raindrop Size Distribution Measurements by Collocated Disdrometers, Journal of Atmospheric and Oceanic Technology, 30, 1672–1690, https://doi.org/10.1175/JTECH-D-12-00163.1, https://doi.org/10.1175/JTECH-D-12-00163.1, 2013.

Tokay, A., Wolff, D. B., and Petersen, W. A.: Evaluation of the New Version of the Laser-Optical Disdrometer, OTT Parsivel2, Journal of Atmospheric and Oceanic Technology, 31, 1276–1288, https://doi.org/10.1175/JTECH-D-13-00174.1, https://doi.org/10.1175/JTECH-D-13-00174.1, 2014.

Tridon, F., Battaglia, A., Kollias, P., Luke, E., and Williams, C. R.: Signal postprocessing and reflectivity calibration of the Atmospheric Radiation Measurement 915-MHz wind profilers, J. Atmos. Oceanic Technol., 30, 1038?1054, 2013.

Williams, C. R., Ecklund, W. L., and Gage, K. S.: Classification of Precipitating Clouds in the Tropics Using 915-MHz Wind Profilers, Journal of Atmospheric and Oceanic Technology, 12, 996–1012, https://doi.org/10.1175/1520-0426(1995)012<0996:COPCIT>2.0.CO;2, https://doi.org/10.1175/1520-0426(1995)012<0996:COPCIT>2.0.CO;2, 1995.

Williams, E., Rosenfeld, D., Madden, N., Gerlach, J., Gears, N., Atkinson, L., Dunnermann, N., Frostom, G., Antonio, M., Biazon, B., Camargo, R., Franca, H., Gomes, A. M., and Lima, M. A.: Contrasting convective regimes over the Amazon: Implications for cloud electrification., J. Geophys. Res., 107, 8082, https://doi.org/10.1029/2001JD000380, 2002.

Yuter, S. E. and Houze, R. A.: Three-dimensional kinematic and microphysical evolution of Florida cumulonimbus. Part II: Frequency distribution of vertical velocity, reflectivity, and differential reflectivity, Mon. Weather Rev., 123, 1941–1963, 1995.

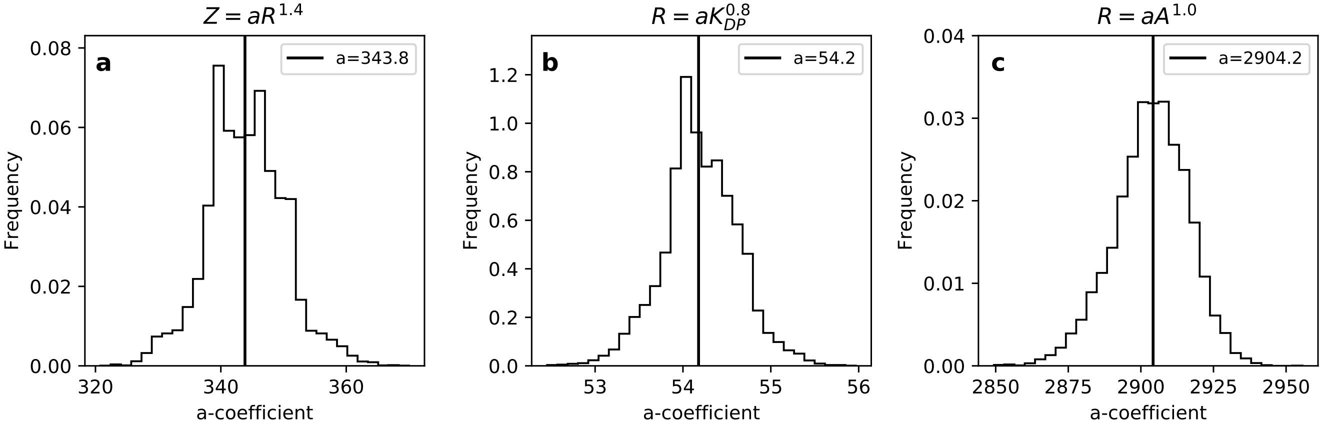

Figure 1. Histograms for *a*-coefficient values from single parameter rainfall relationships (a) $R(Z)$, (b) $R(K_{DP})$, and (c) $R(A)$, calculated using least square method under the assumption of *a* fixed *b*-coefficient from random sampling of half of the dataset (5000 times), for the S-band wavelength. The black vertical lines represent the a-coefficient calculated based on the whole dataset.

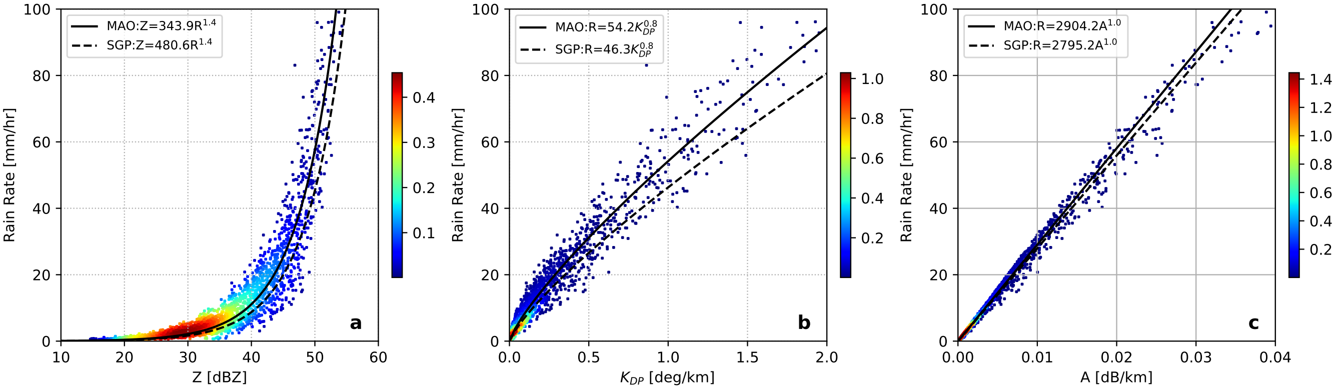

Figure 2. Scatter plots of (a) Z, (b) K_{DP}, and (c) A versus rain rate and overlaid associated relationship fits using least square method for Amazon (~~AM~~ MAO, solid lines) and SGP-Oklahoma (SGP, dashed lines) sites, for the S-band wavelength. Density ~~calculated using a kernel function~~ is shown in colors.

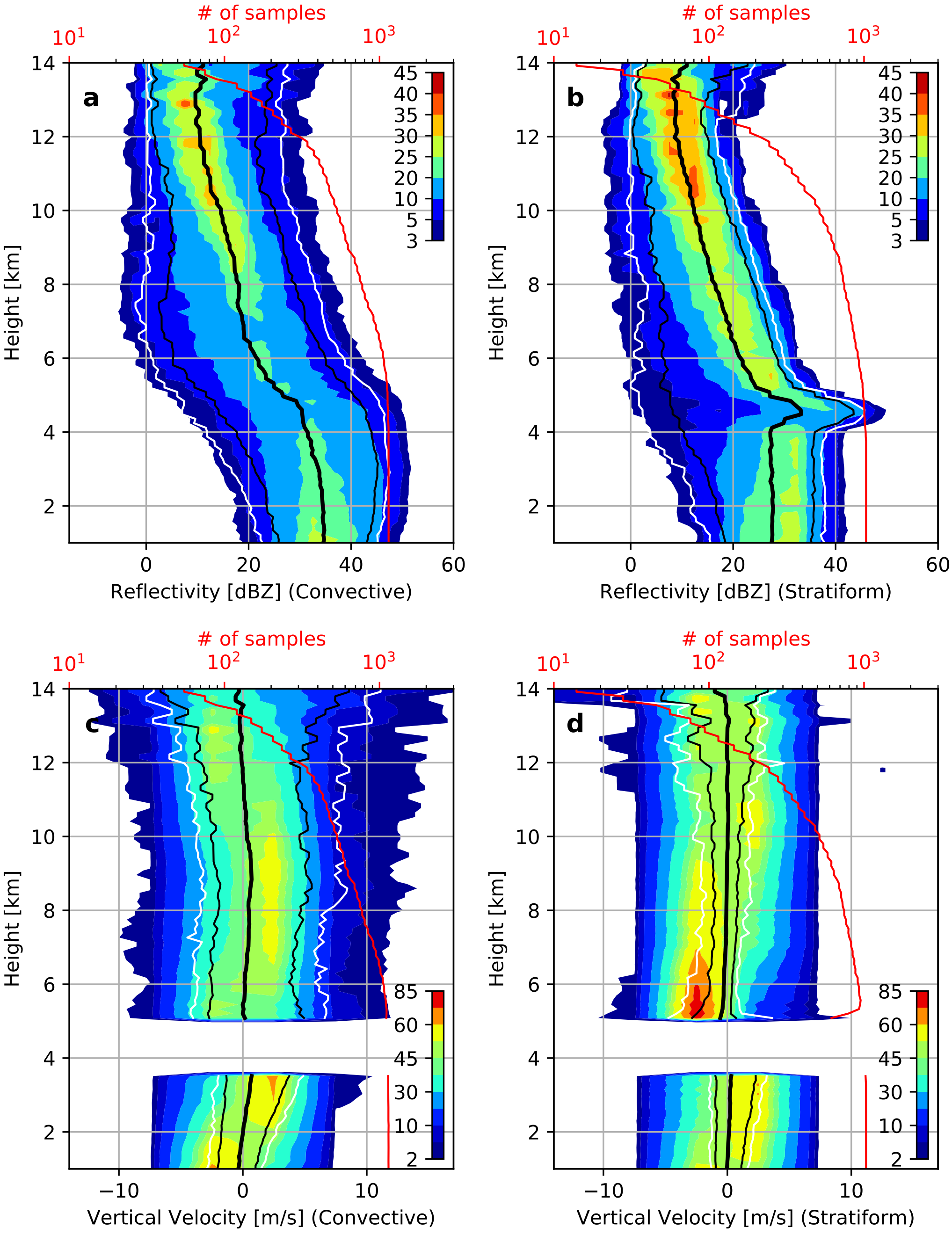

Figure 3. Contoured frequency altitude display histograms (CFADs) for the entire Amazon dataset with confidence intervals, median (thick black lines), 90th (thin black lines) and 95th percentile (white lines), for RWP convective and stratiform reflectivity profiles (a, b) and vertical velocity retrievals (c, d). The number of profiles of each situation is shown as a red line.

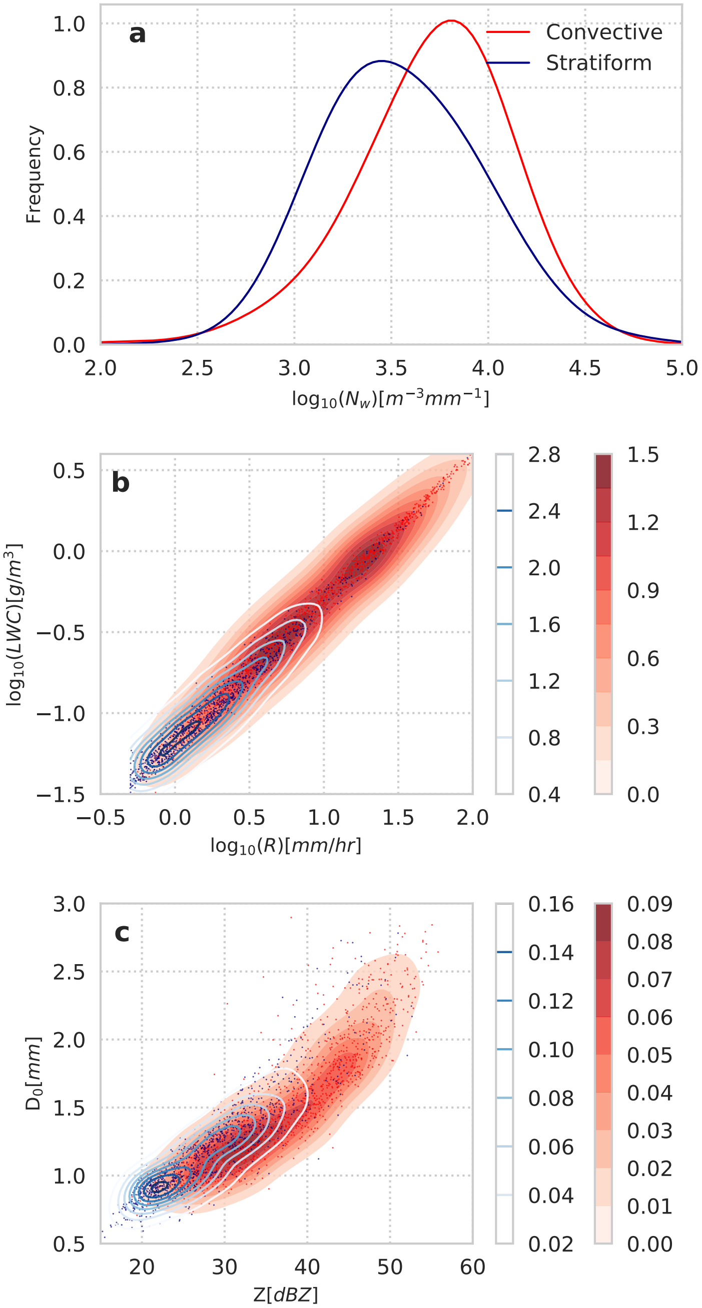

Figure 4. Histograms associated with RWP classification based convective (red) and stratiform (blue) DSDs in terms of N_w (a), LWC versus R behaviors (b), and D_0 scaling according to Z (c). Density is shown in colors.

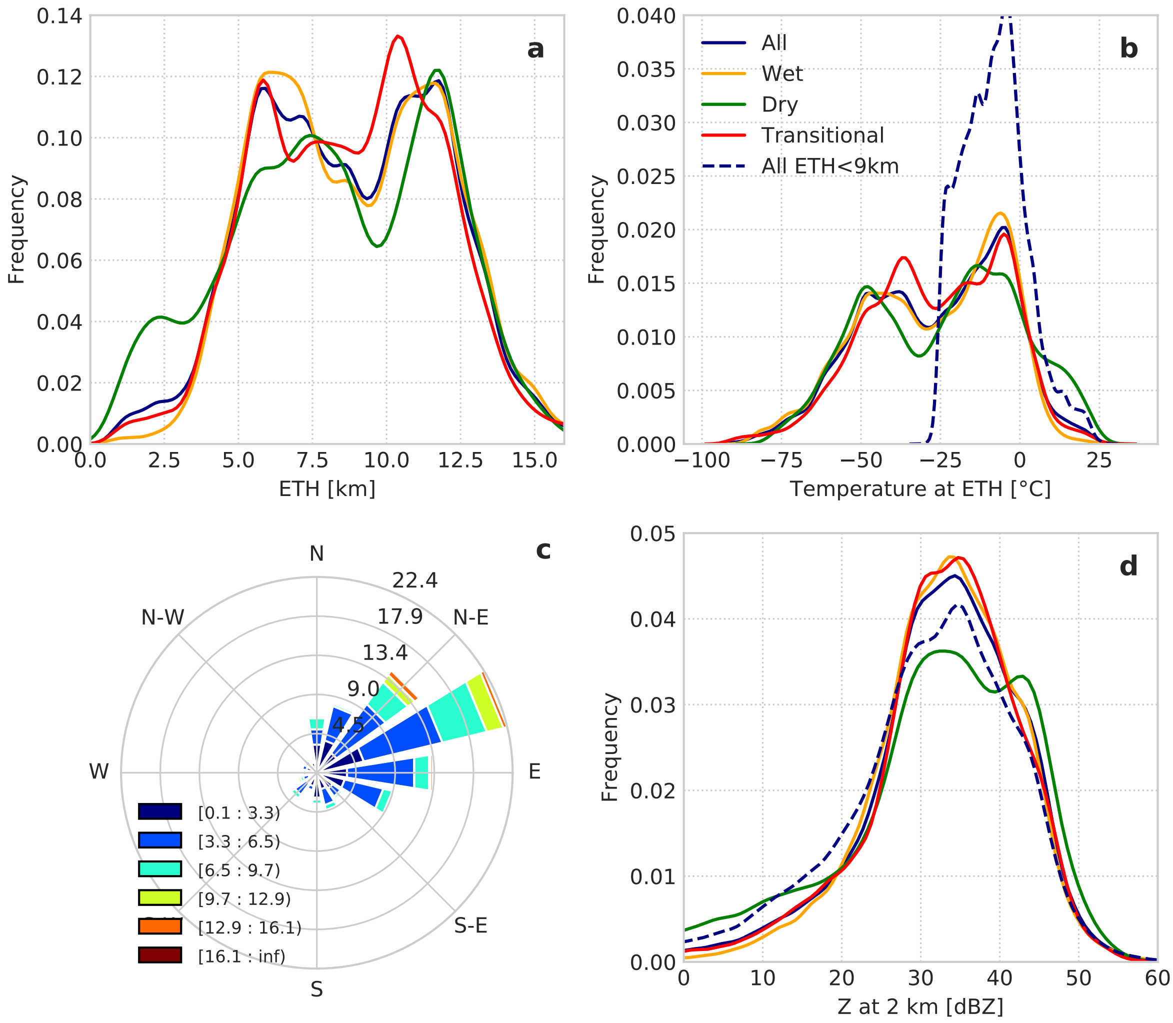

Figure 5. Histograms associated with RWP classification based convective DSDs in terms of ETH (a), temperature at ETH (b), and Z at 2 km (d) for All, Dry, Wet, Transitional seasons, as well as the congestus for all the seasons. The wind rose (c) is also shown for all the seasons.

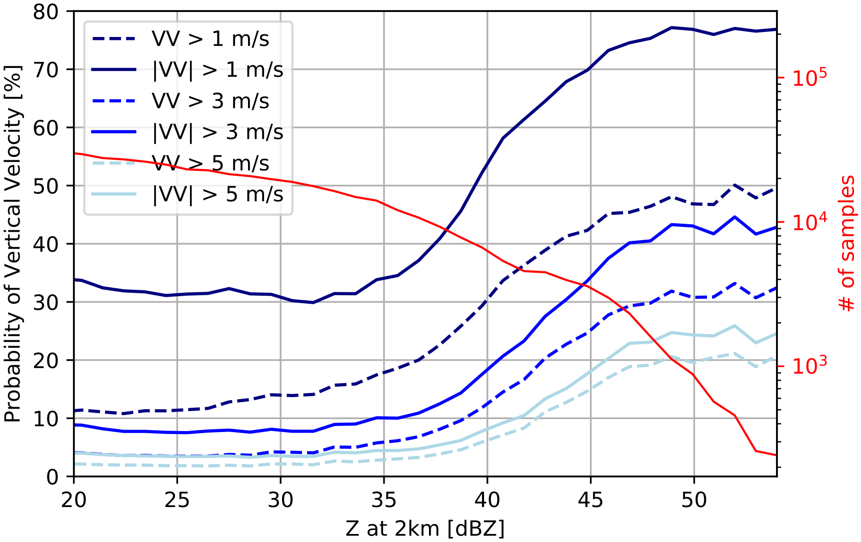

Figure 6. The frequency for observing a given vertical velocity (across all levels, > 1 ms^{-1} in navy, > 3 ms^{-1} in dark green, > 5 ms^{-1} in light green) as a function of a 2 km RWP reflectivity. The number of samples (for |VV| > 1 ms^{-1}) are displayed as a red line.

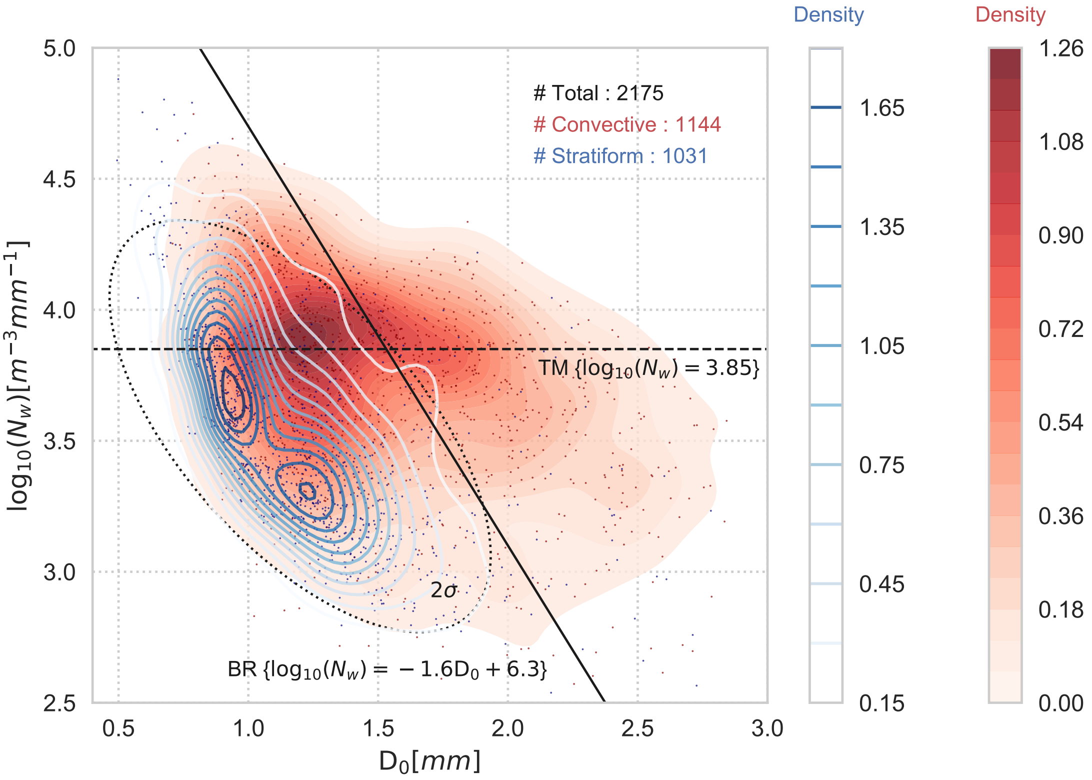

Figure 7. Scatter plot of $\log_{10}(N_w)$ versus D_0 from PARSIVEL disdrometer, overlaid by the contours representing the RWP-based classifications for convective (red colors) and stratiform (blue lines) precipitating columns. The ellipse conveys the two-sigma confidence interval (dotted line) for those regions containing RWP-based stratiform DSDs. The convective-stratiform regime segregation concepts in Bringi et al. (2003, BR) and in Thompson et al. (2015, TM) are presented as a solid black line and dashed black line, respectively.

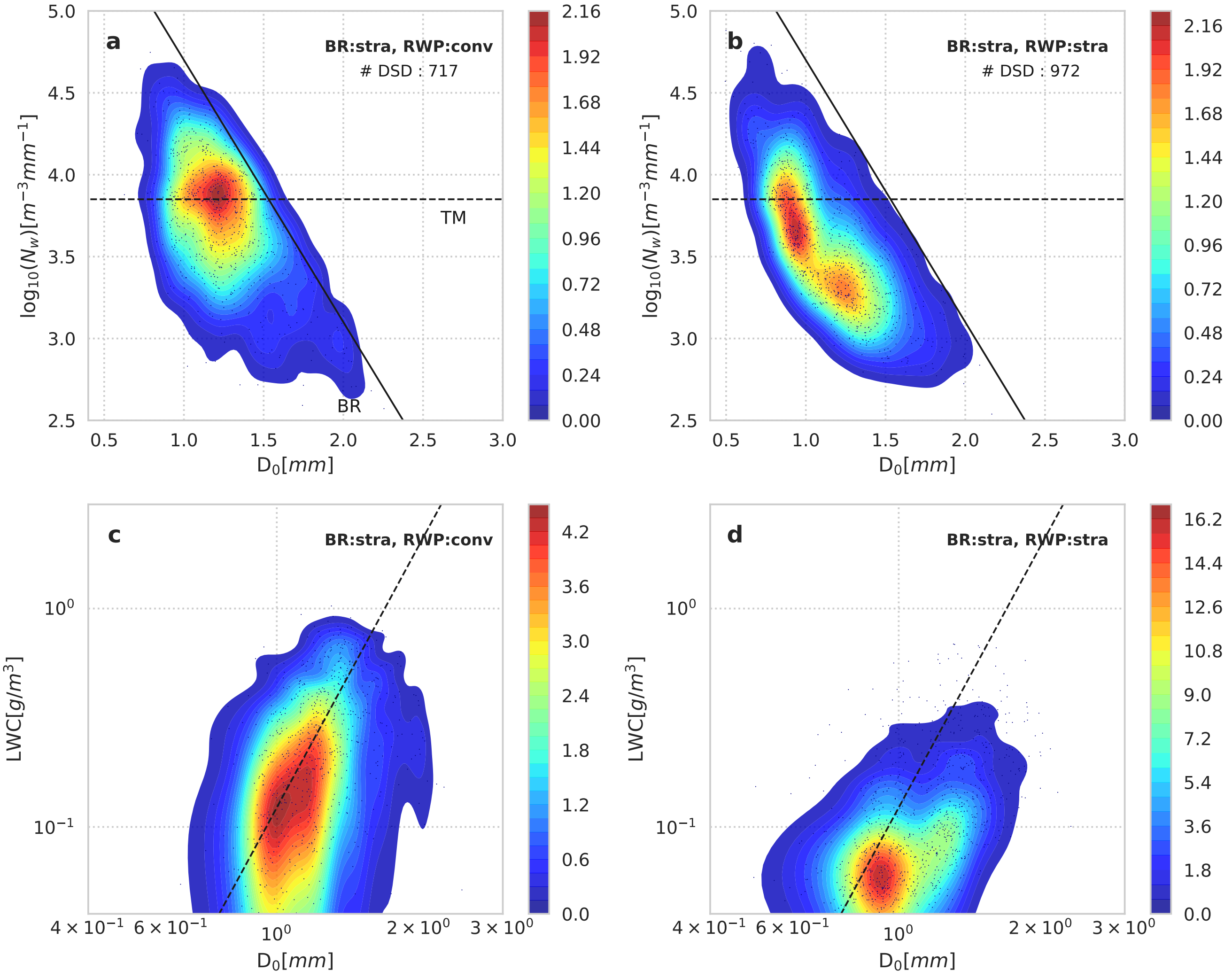

Figure 8. Scatter plots of $\log_{10}(N_w)$ versus D_0 and LWC versus D_0 for BR-based stratiform DSDs (~~probability~~ density in colors). DSDs identified as convective/stratiform by the RWP are shown in (a, c)/(b, d). ~~BR line and TM line are shown as a solid black line and dashed black line, respectively.~~

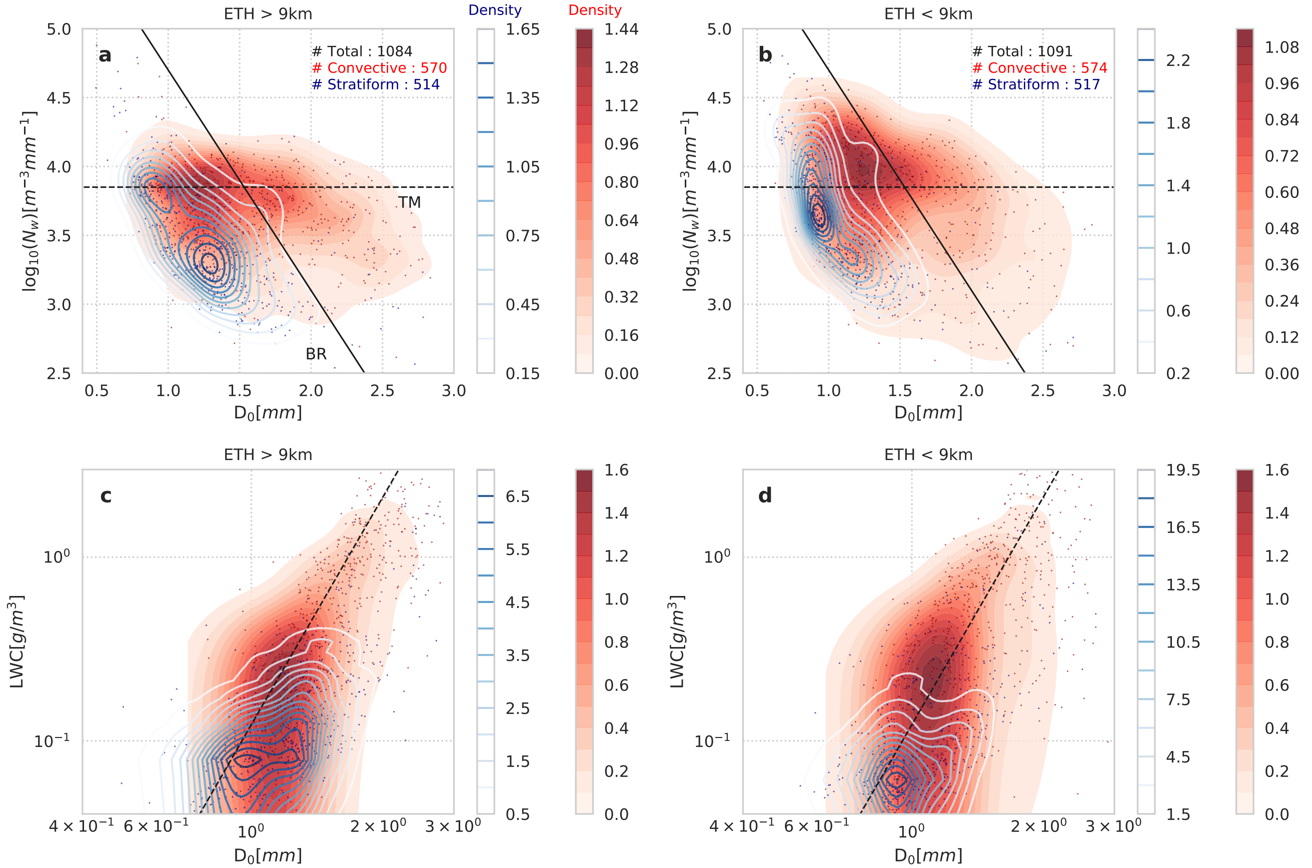

Figure 9. Scatter plots of $\log_{10}(N_w)$ versus D_0 and LWC versus D_0, overlaid by the contours representing the RWP-based classifications for convective (red colors) and stratiform (blue lines) precipitating columns, for ETH > 9 km (a, c) and ETH < 9 km (b, d) situations. ~~BR line and TM line are shown as a solid black line and dashed black line, respectively.~~

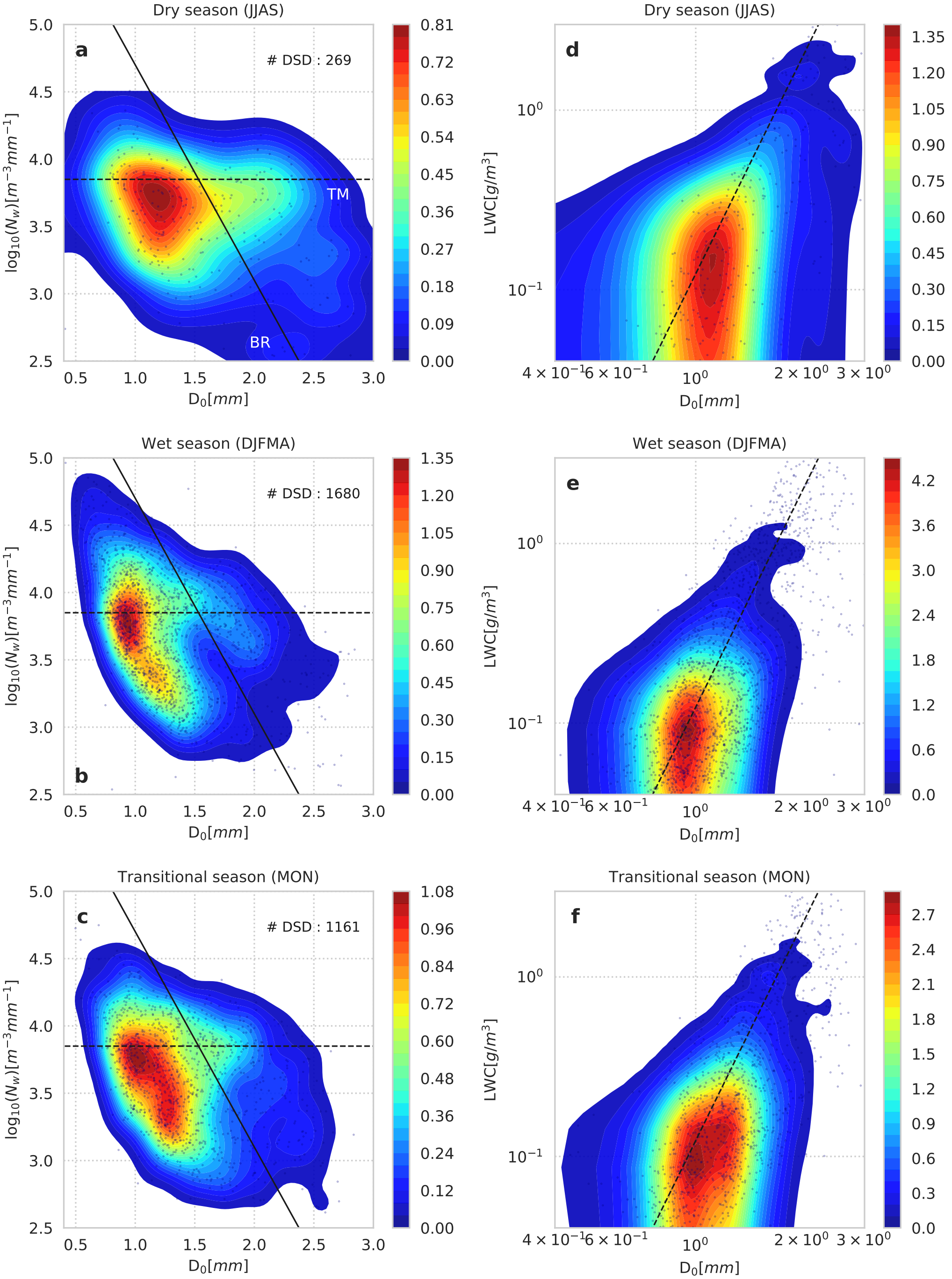

Figure 10. Scatter plots of $\log_{10}(N_w)$ versus D_0 and LWC versus D_0 for Dry (a, d), Wet (b, e) , and Transitional (c, f) seasons (~~probability~~ density in colors). ~~BR line and TM line are shown as a solid black line and dashed black line, respectively.~~

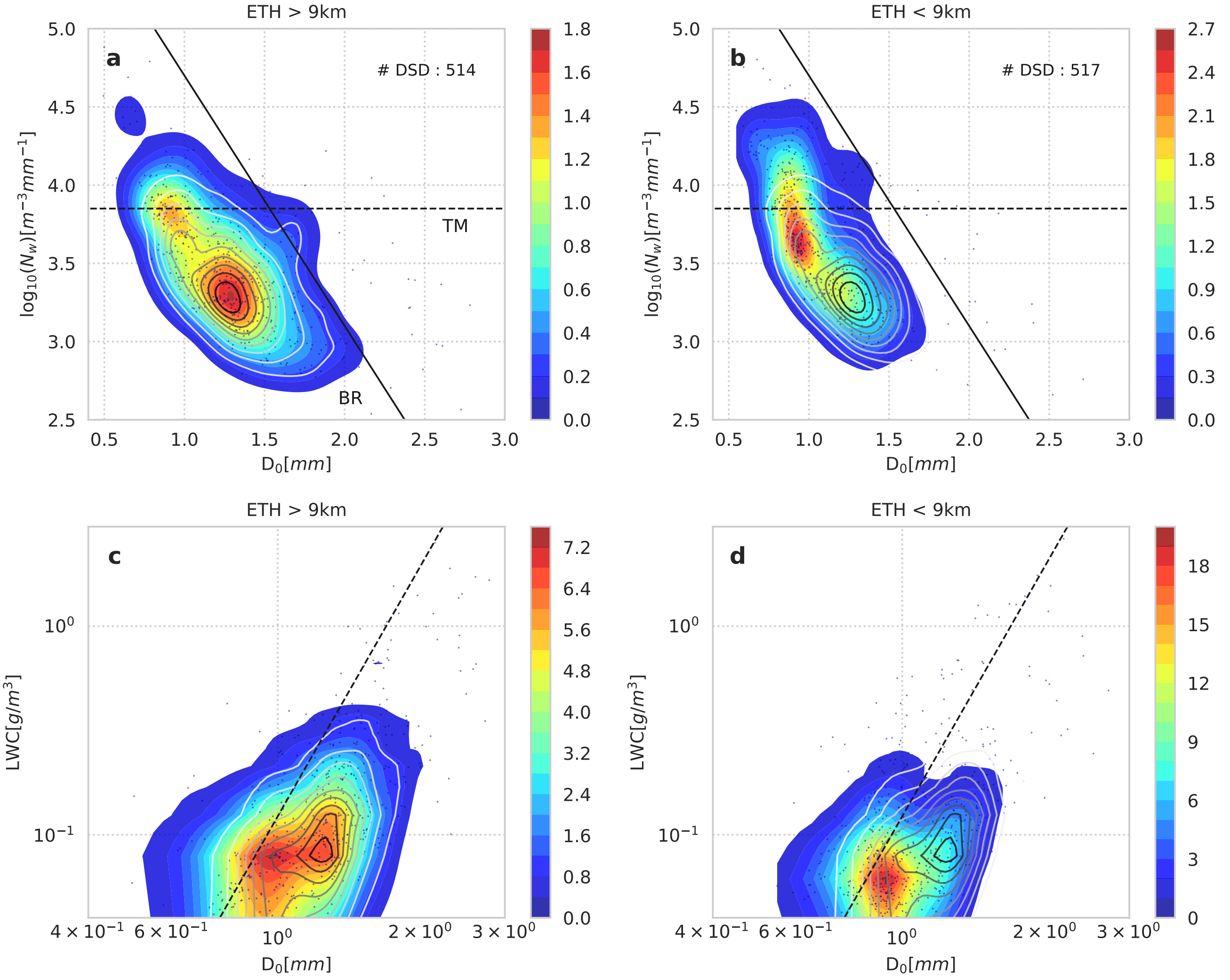

Figure 11. Scatterplots of $\log_{10}(N_w)$ versus D_0 and LWC versus D_0 for RWP-based stratiform DSDs (~~probability~~ density in colors), for ETH < 9 km (a, c) and ETH > 9 km (b, d) DSDs. The overlaid black contours represent the RWP-based classifications for stratiform with bright band precipitating columns. ~~BR line and TM line are shown as a solid black line and dashed black line, respectively.~~

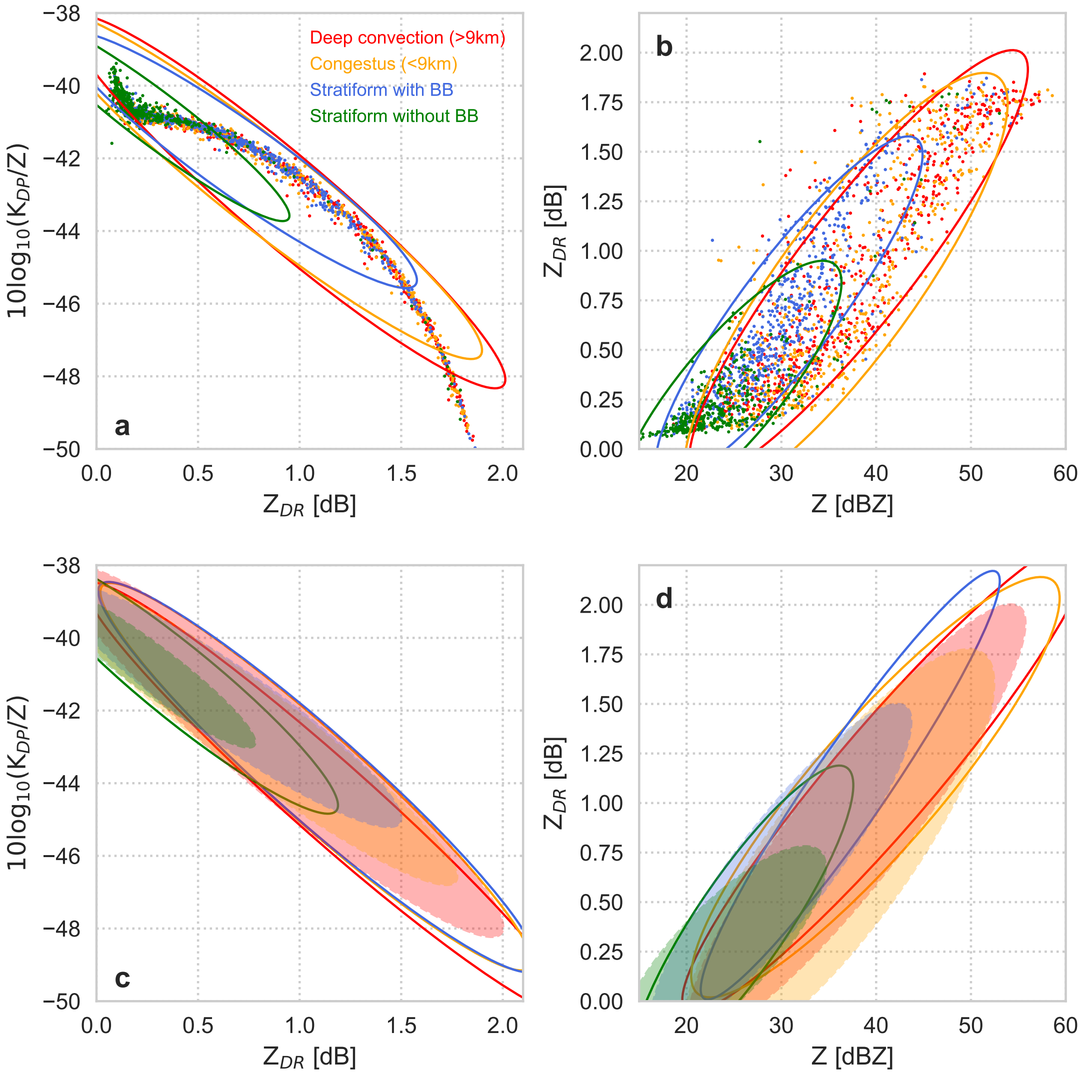

Figure 12. Scatter plots of Z_{DR} versus 10log$_{10}$(K_{DP}/Z) and Z versus Z_{DR} for the various regimes, deep convection, congestus, stratiform with bright band and stratiform without bright band identified by the RWP classifications (a, b). The ellipses convey the two-sigma confidence interval for corresponding regimes. The Wet (shaded ellipses)/Dry (ellipses) season segregations (c, d) are presented in c and d.

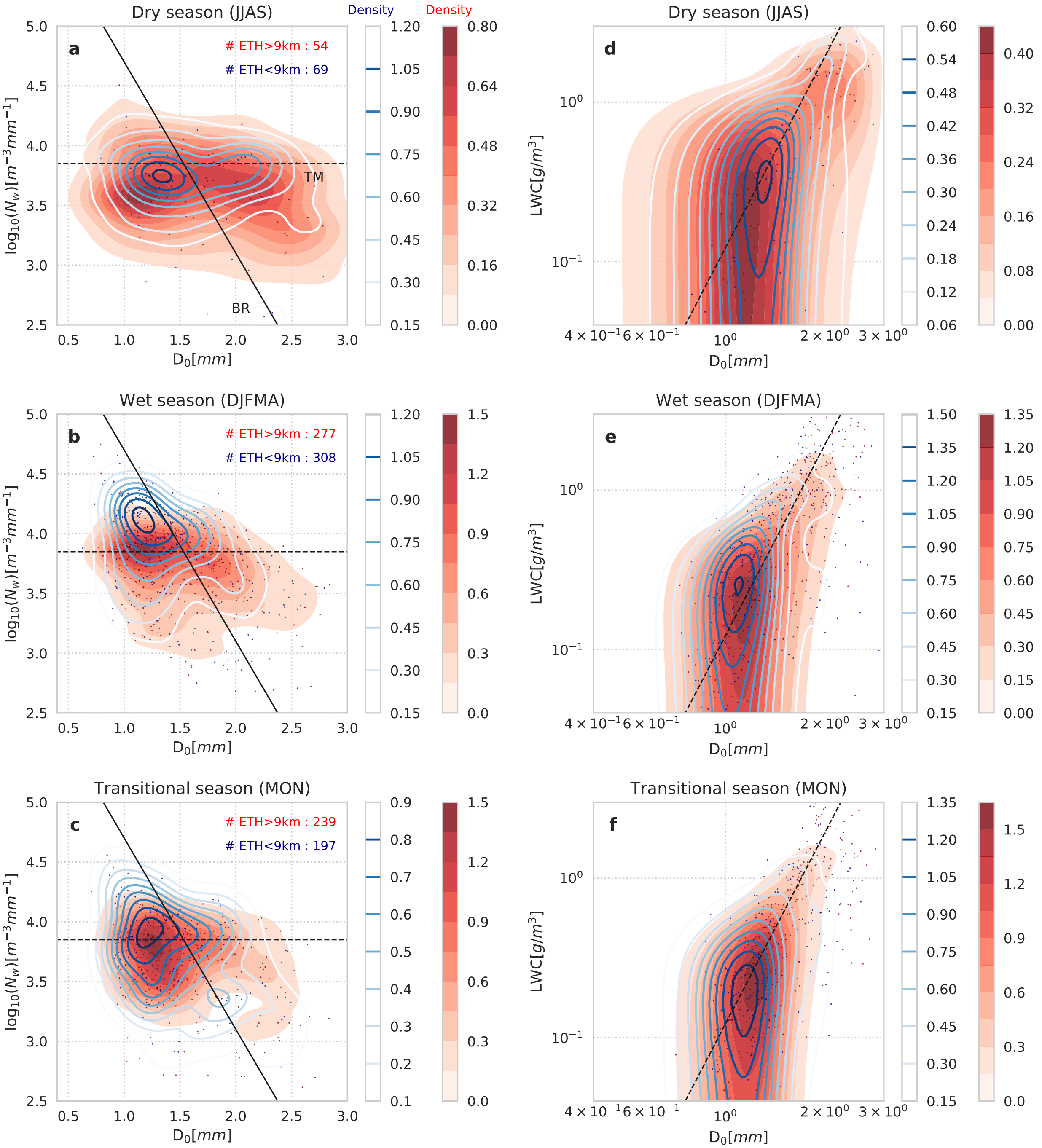

Figure 13. Scatter plots of $\log_{10}(N_w)$ versus D_0 and LWC versus D_0 for RWP-based convective DSDs, for Dry (a, d), Wet (b, e) , and Transitional (c, f) seasons. The contours represent the congestus (ETH < 9 km, blues) and deep (ETH > 9 km, reds) convective DSDs. ~~BR line and TM line are shown as a solid black line and dashed black line, respectively.~~

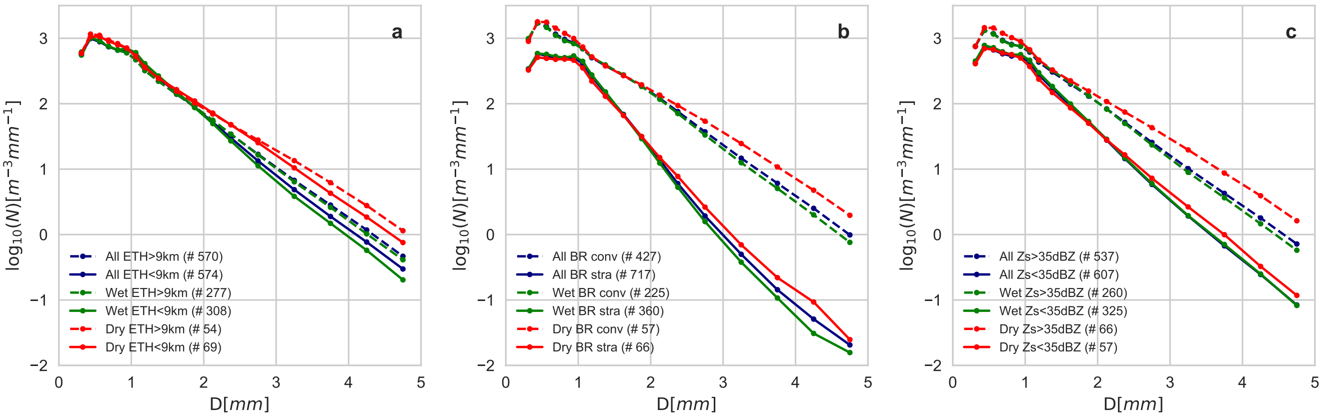

Figure 14. Averaged RWP-based convective DSDs for congestus (ETH < 9 km) and deep (ETH > 9 km) DSDs (a), for convective and stratiform DSDs depending on the BR separation (b), as well as for those having Z (at surface) < 35 dBZ and Z > 35 dBZ (c), for All, Dry and Wet seasons.

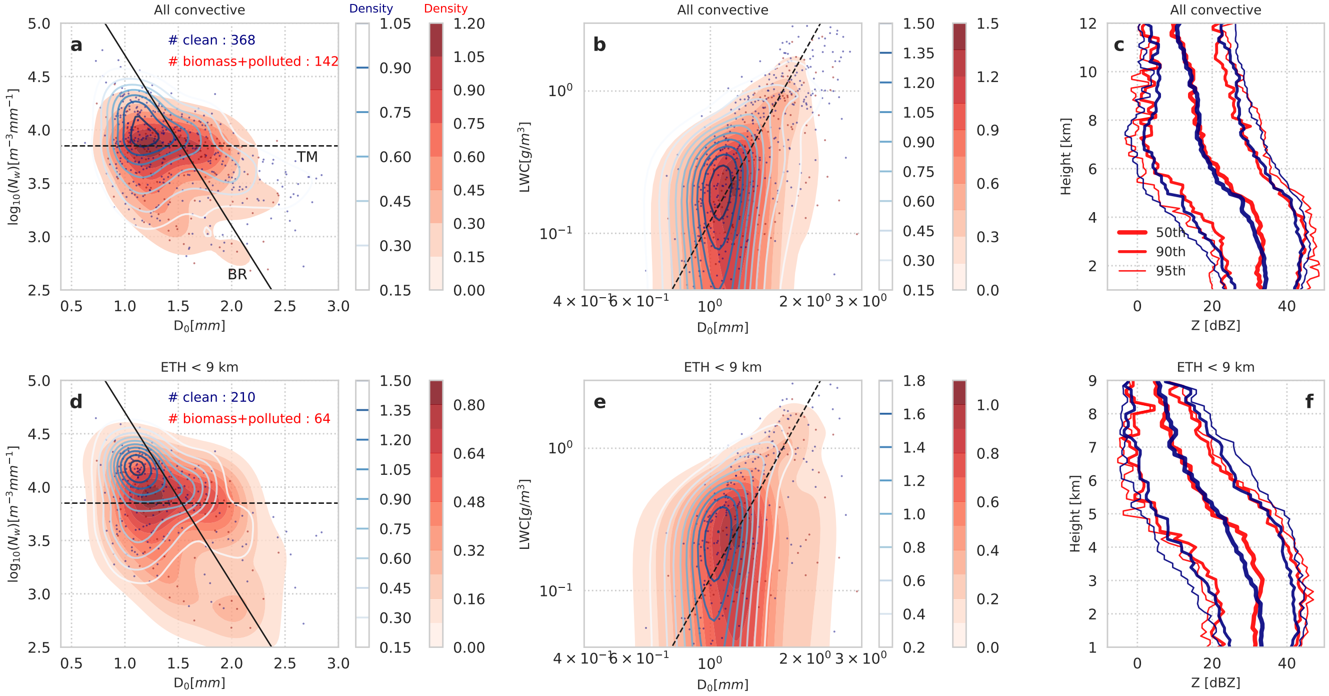

Figure 15. Scatter plots of $\log_{10}(N_w)$ versus D_0 and LWC versus D_0 for RWP-based convective DSDs under the Wet season (a, b), as well as for only congestus convective DSDs (d, e), contouring the clean (blues) and polluted (reds) conditions. The corresponding composite median, 90th and 95th percentile RWP Z profile behaviors under the clean (blue) and polluted (red) conditions are shown in c and f.

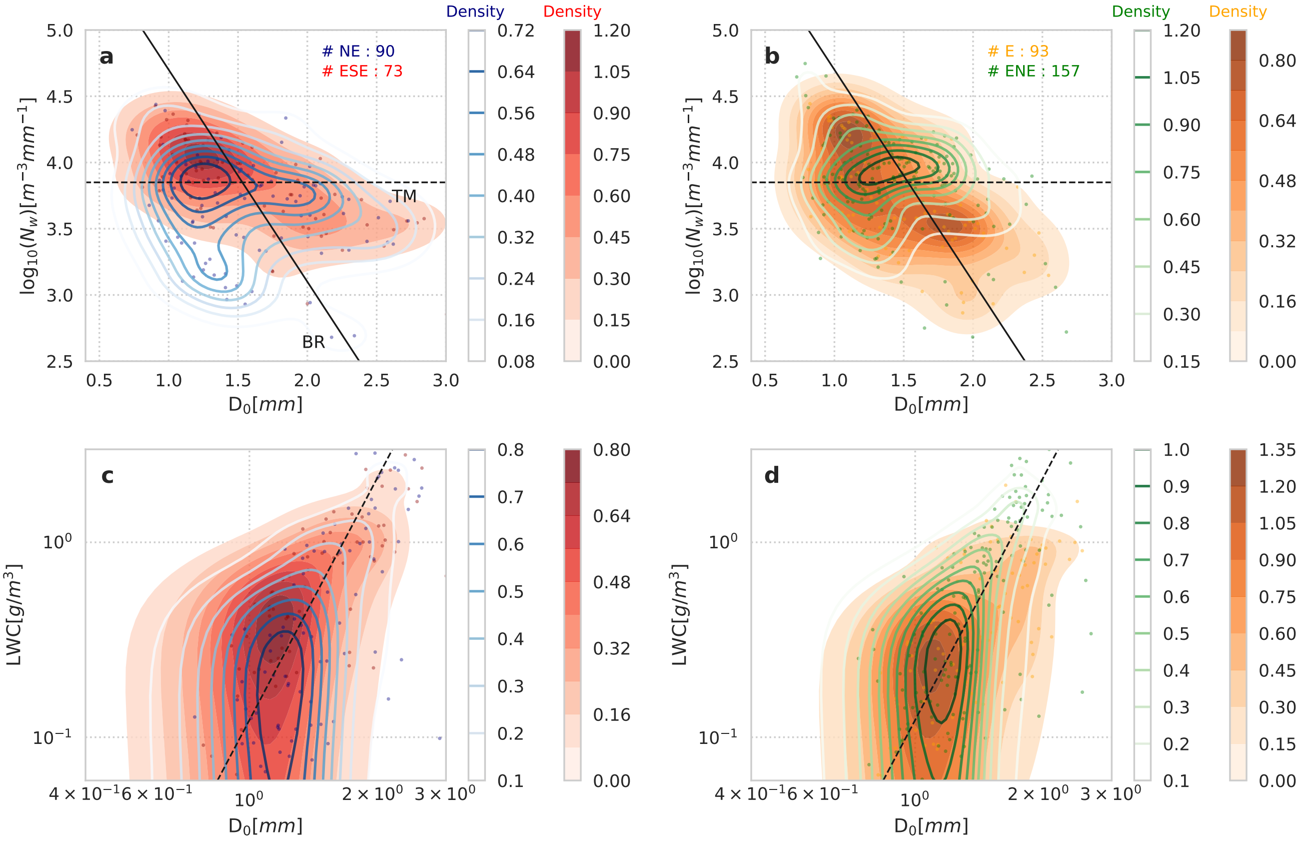

Figure 16. Scatter plots of $\log_{10}(N_w)$ versus D_0 and LWC versus D_0 for Wet season DSDs on the ambient wind directions, northeasterly/east-southeasterly (NE (blues)/ESE (reds)) and east/east-northeast (E (oranges)/ENE (greens)).

Table 1. A summary of 5-minute DSD parameter breakdowns for number of DSDs, rain rate R, median volume drop size D_0, normalized DSD intercept parameter N_w, reflectivity Z at S-band, and liquid water content LWC, filtered according to rainfall rate intervals, for All, Wet, and Dry seasons.

R[mmhr^{-1}]	No. DSD		<R>[mmhr^{-1}]		<D$_0$>[mm]		<N$_w$>[m^{3}mm^{-1}]		<Z>[dBZ]		<LWC>[gm^{-3}]	
All (Total rainfall = 2597 mm for MAO Dataset, 694 mm for SGP Dataset)												
	MAO	SGP	MAO	SGP	MAO	SGP	MAO	SGP	MAO	SGP	MAO	SGP
0.5-2	1080	676	1.15	1.17	1.01	0.97	6580	8882	24.1	24.1	0.08	0.08
2-4	582	337	2.86	2.87	1.24	1.26	6525	4718	30.5	30.9	0.17	0.15
4-6	294	148	4.83	4.83	1.34	1.46	7621	4454	33.7	34.7	0.27	0.23
6-10	292	116	7.66	7.56	1.49	1.73	7445	3873	36.5	38.5	0.39	0.34
10-20	339	85	14.61	14.29	1.70	1.95	6913	4333	40.8	42.3	0.69	0.61
20-40	289	61	27.79	28.48	1.90	2.16	6948	4543	44.9	45.9	1.21	1.08
40-60	93	19	48.95	47.89	2.07	2.24	7699	5502	48.4	49.0	2.03	1.82
Wet season (Total rainfall = 1245 mm for MAO Dataset)												
0.5-2	649		1.14		0.99		6892		23.7		0.08	
2-4	301		2.88		1.19		7851		30.1		0.17	
4-6	148		4.80		1.33		8933		33.5		0.27	
6-10	147		7.73		1.49		8295		36.1		0.39	
10-20	162		14.78		1.65		8149		40.4		0.72	
20-40	147		27.57		1.86		7666		44.7		1.23	
40-60	44		49.02		2.04		8547		48.1		2.05	
Dry season (Total rainfall = 366 mm for MAO Dataset)												
0.5-2	73		1.19		1.06		4453		24.9		0.08	
2-4	33		2.79		1.32		4694		30.9		0.15	
4-6	24		4.76		1.29		7417		33.1		0.27	
6-10	31		7.72		1.53		5045		37.7		0.38	
10-20	34		14.92		1.89		4151		42.5		0.65	
20-40	30		28.60		2.13		4275		46.4		1.16	
40-60	14		49.35		2.24		5349		49.3		1.93	

Table 2. Radar rainfall and self-consistency relations for GoAmazon2014/5 dataset, for the cumulative dataset All, Wet, and Dry seasons, as well as convective and stratiform precipitation as based on RWP classifications. Coefficients estimated at S, C, and X-band radar wavelengths.

Wavelength		R(Z) (T=20°C)	$R(K_{DP})$ (T=20°C)	R(A) (T=20°C)	R(A) (T=10°C)
S band	All	$Z = 343.9R^{1.4}$	$R = 54.2K_{DP}^{0.8}$	$R = 2904.2A^{1.0}$	$R = 2227.6A^{1.0}$
	Wet season	$Z = 329.5R^{1.4}$	$R = 55.2K_{DP}^{0.8}$	$R = 2949.6A^{1.0}$	$R = 2265.1A^{1.0}$
	Dry season	$Z = 388.3R^{1.4}$	$R = 51.5K_{DP}^{0.8}$	$R = 2732.3A^{1.0}$	$R = 2090.5A^{1.0}$
	Convective	$Z = 339.9R^{1.4}$	$R = 54.6K_{DP}^{0.8}$	$R = 2895.0A^{1.0}$	$R = 2219.6A^{1.0}$
	Stratiform	$Z = 385.8R^{1.4}$	$R = 51.1K_{DP}^{0.8}$	$R = 2867.1A^{1.0}$	$R = 2202.0A^{1.0}$
C band	All	$Z = 289.0R^{1.4}$	$R = 30.6K_{DP}^{0.8}$	$R = 287.8A^{0.9}$	$R = 239.4A^{0.9}$
	Wet season	$Z = 280.6R^{1.4}$	$R = 31.3K_{DP}^{0.8}$	$R = 314.4A^{0.9}$	$R = 258.3A^{0.9}$
	Dry season	$Z = 314.8R^{1.4}$	$R = 28.5K_{DP}^{0.8}$	$R = 242.1A^{0.9}$	$R = 203.4A^{0.9}$
	Convective	$Z = 281.6R^{1.4}$	$R = 30.7K_{DP}^{0.8}$	$R = 278.4A^{0.9}$	$R = 232.3A^{0.9}$
	Stratiform	$Z = 339.8R^{1.4}$	$R = 29.5K_{DP}^{0.8}$	$R = 290.6A^{0.9}$	$R = 239.7A^{0.9}$
X band	All	$Z = 261.4R^{1.6}$	$R = 21.5K_{DP}^{0.8}$	$R = 41.4A^{0.8}$	$R = 43.0A^{0.8}$
	Wet season	$Z = 239.1R^{1.6}$	$R = 21.6K_{DP}^{0.8}$	$R = 42.7A^{0.8}$	$R = 43.9A^{0.8}$
	Dry season	$Z = 303.2R^{1.6}$	$R = 21.1K_{DP}^{0.8}$	$R = 38.2A^{0.8}$	$R = 40.0A^{0.8}$
	Convective	$Z = 250.2R^{1.6}$	$R = 21.6K_{DP}^{0.8}$	$R = 41.0A^{0.8}$	$R = 43.0A^{0.8}$
	Stratiform	$Z = 318.5R^{1.6}$	$R = 19.6K_{DP}^{0.8}$	$R = 40.8A^{0.8}$	$R = 41.3A^{0.8}$
Self-consistency (T=20°C)					
S band	All	$Z = 45.6 + 10.04\log(K_{DP}) + 3.20Z_{DR}$			
	Wet season	$Z = 45.7 + 10.10\log(K_{DP}) + 3.17Z_{DR}$			
	Dry season	$Z = 45.6 + 10.05\log(K_{DP}) + 3.16Z_{DR}$			
C band	All	$Z = 43.3 + 10.12\log(K_{DP}) + 1.96Z_{DR}$			
	Wet season	$Z = 43.3 + 10.18\log(K_{DP}) + 1.94Z_{DR}$			
	Dry season	$Z = 43.4 + 10.12\log(K_{DP}) + 1.82Z_{DR}$			
X band	All	$Z = 38.6 + 9.54\log(K_{DP}) + 4.62Z_{DR}$			
	Wet season	$Z = 38.7 + 9.54\log(K_{DP}) + 4.52Z_{DR}$			
	Dry season	$Z = 38.7 + 9.80\log(K_{DP}) + 4.89Z_{DR}$			